

## ABSTRACT

Title of Thesis:                   COUPLING REDUCTION USING  
ELECTROMAGNETIC BAND GAP  
STRUCTURES IN ENCLOSURES AND  
CAVITIES

Baharak Mohajer Iravani  
Master of Science, 2004

Thesis Directed By:           Dr. Omar M. Ramahi, Department of  
Mechanical/Electrical Engineering

Electromagnetic Interference (EMI) in electronic devices is one of the major challenges in the design of high-speed electronic packages. These challenges are intensified by the increase in the level of system integration and the ever-increasing operating frequency of microprocessors. EMI takes place at different levels including the package, board, component and chip. The physical mechanism behind electromagnetic interference is the coupling of energy between different EM sources. This coupling can be either conducted or radiated. However, regardless of the coupling mechanism, surface currents are needed to support the field that eventually radiates, which constitute the electromagnetic interference in the first place. Minimizing these surface currents is considered a fundamental and critical step in minimizing EMI. In this work, novel strategies are proposed to confine surface currents in enclosures and cavities. Unlike the traditional use of lossy materials and absorbers, which suffers from considerable disadvantages including mechanical and

thermal reliability leading to limited life time, we consider the use of electromagnetic Band Gap (EBG) structures which are inherently suited for surface current suppression. The effectiveness of the EBG as an EMI suppresser in enclosures, chasses and cavities will be demonstrated using numerical simulations.

# **COUPLING REDUCTION USING ELECTROMAGNETIC BAND GAP STRUCTURES IN ENCLOSURES AND CAVITIES**

By

Baharak Mohajer Iravani

Thesis submitted to the Faculty of the Graduate School of the  
University of Maryland, College Park, in partial fulfillment  
of the requirements for the degree of  
Master of Science  
2004

Advisory Committee:  
Associate Professor Omar Ramahi, Chair  
Professor Neil Goldsman  
Professor Agis Iliadis

© Copyright by  
Baharak Mohajer Iravani  
2004

## Dedication

**This work is dedicated to my parents.**

## Acknowledgements

I would like to thank my parents for their encouragement and support.

I would like to thank Dr. Ramahi who guided, encouraged and supported me through this project.

I would like to thank Dr. Goldsman and Dr. Iliadis whom accepted to serve on my committee.

I would like to thank my colleagues Mehdi, Mohammad, Shahrooz, Lin and Xin for helpful discussion and comments and providing help during experiments and measurements.

This research was supported in part by DoD MURI Program on Effects of Radio frequency Pulses on Electronic Circuits and Systems under AFSOR Grant F496200110374. Also funding of this project was provided in part by the CALCE Electronics Products and Systems Center at the University of Maryland College Park

# Table of Contents

|   |     |
|---|-----|
| Dedication .....  | ii  |
| Acknowledgements .....  | iii |
| Table of Contents .....   | iv  |
| List of Tables .....  | v   |
| List of Figures .....   | vi  |
| Chapter 1 : Introduction .....  | 1   |
| Chapter 2 : Problem and Challenges .....  | 5   |
| Chapter 3 : Classical Solutions .....   | 8   |
| 3.1. Electromagnetic Interference Reduction in Packages and Enclosures .....              | 8   |
| 3.1.1. Change in configuration of openings .....  | 9   |
| 3.1.2. Implementing Lossy Material to Enclosures and Openings .....                       | 10  |
| 3.1.3. Design of Package according to PCB features .....                                  | 11  |
| 3.2. Electromagnetic Interference Reduction in Cavity Backed Slot Antennas .....          | 12  |
| 3.2.1. Implementing Lossy Materials .....   | 17  |
| 3.2.2. Slit on the Ground Plane .....   | 18  |
| 3.2.3. Change in Configuration .....  | 21  |
| 3.2.4. Separation Distance .....  | 23  |
| Chapter 4 : Electromagnetic Band Gap (EBG) Materials .....                                | 24  |
| 4.1. EBG Structures .....   | 24  |
| 4.2. Design of EBG Structures .....   | 28  |
| 4.2.1. Scattering parameters .....  | 29  |
| 4.2.2. Dispersion Diagram .....   | 30  |
| 4.3. Surface Wave .....   | 34  |
| 4.4. EM wave mitigation using EBG materials .....   | 39  |
| 4.4.1. Antenna .....  | 39  |
| 4.4.2. Power planes and Printed Circuit Boards .....                                      | 44  |
| 4.4.3. Signal Integrity on PCBs .....   | 46  |
| Chapter 5 : Application of EBG Materials for EM Noise Suppression .....                   | 47  |
| 5.1. New EMI Shielding Approach in Enclosures Using EBG .....                             | 47  |
| 5.1.1. Methodology .....  | 47  |
| 5.1.2. Numerical Simulation and Validation .....  | 50  |
| 5.2. Surface Wave Suppression in Cavity Backed Slot Antennas .....                        | 55  |
| 5.2.1. Methodology .....  | 55  |
| 5.2.2. Numerical Simulation and Validation .....  | 60  |
| 5.3. Effect of two different Configurations of the same EBG Pattern on the Band Gap ..... | 70  |
| 5.3.1. Configurations .....   | 70  |
| 5.3.2. Simulation Result .....  | 70  |
| Chapter 6 : Summary and Future work .....   | 72  |
| Bibliography .....  | 74  |

## List of Tables

|  |    |
|--|----|
| Table 5. I. The specification of unit cell of the EBG pattern.....   | 50 |
| Table 5. II. The specification of unit cell of the EBG pattern ..... | 60 |



## List of Figures

|  |    |
|--|----|
| Figure 3. 1. Geometry of the cavity-backed slot antenna .....  | 13 |
| Figure 3. 2. Return loss of CBS antenna specified in Figure 3. 1 by measurement and FDTD simulation .....  | 13 |
| Figure 3. 3. Air-filled rectangular CBS antenna fed with probe oriented in the y-direction. (a) Perspective view, (b) top view and (c) side view of antenna.....   | 15 |
| Figure 3. 4. Geometry of two identical CBS antennas mounted on rectangular ground plane (for antenna specification see Figure 3. 3), (a) perspective view and (b) top view.....  | 16 |
| Figure 3. 5 Magnitude of $S_{11}$ of two identical CBS antennas mounted on a ground plane. These data extracted by measurement and numerical analysis (The numbers in front of FDTD method show order of accuracy in time and space domains). For antenna specification see Figure 3. 3..... | 17 |
| Figure 3. 6. Top view of CBS antennas on a ground plane with GDS superstrate in between .....  | 18 |
| Figure 3. 7. Both measured and simulated coupling interference between two CBS antennas with and without presence of lossy superstrate in three cases of (a) 1.5 mm thick GDS, (b) 3.0mm thick GDS, (c) 4.5 mm thick GDS.....  | 19 |
| Figure 3. 8. Ground plane with slit to reduce mutual coupling between antennas .....   | 20 |
| Figure 3. 9. Coupling with a different slits on the ground plane .....   | 21 |
| Figure 3. 10. Top view of two CBS antennas with (a) E-plane and (b) H-plane configuration .....  | 22 |
| Figure 3. 11. Coupling between two CBS antennas oriented in different directions..   | 22 |
| Figure 3. 12. Coupling between two CBS antennas for different separation distances .....   | 23 |
| Figure 4. 1. Geometry of EBG Ground plane (a) perspective view (b) top view .....  | 25 |
| Figure 4. 2.(a) $S_{\text{params}}$ between two ports inside the parallel plates filled with EBG structures, (b) magnitude of electric field inside the parallel plates at 6.6 GHz, (c) surface current on the plate at 6.6 GHz.....   | 26 |
| Figure 4. 3 (a) Side view of EBG structure, (b) Equivalent circuit model of (a) .....  | 28 |
| Figure 4. 4. A setup for extracting band gap of EBG structures using S-parameters, coupled field between ports (i.e. SMA connectors) which positioned across the EBG structures illustrates band stop.....   | 30 |
| Figure 4. 5.(a) Magnitude of $S_{12}$ and (b) Dispersion Diagram of parallel plate waveguide loaded by EBG structure. Specification of EBG is: patch of 10 x 10 mm, gap of .4 mm, via with radius of .4 mm, substrate with $\epsilon_r = 4.4$ and height of 1.54 mm.....                     | 31 |
| Figure 4. 6. shows a unit cell of EBG material and the boundary setting. Also Brillouin triangle is displayed in this figure. Using this setup we extract dispersion diagram which is used to specify band gap .....   | 32 |
| Figure 4. 7. Top view of a unit cell of EBG structure with periodic square patch of length a and gap length of g.....  | 32 |

|   |    |
|---|----|
| Figure 4. 8. Dispersion diagram of an EBG structure, in this structure the band stop is extended from 11.9 to 17.3 GHz.....   | 34 |
| Figure 4. 9. A rectangular surface for computing impedance surface .....  | 35 |
| Figure 4. 10. Propagation of surface wave on an interference of two dissimilar materials.....   | 37 |
| Figure 4. 11.(a) E-plane coupled probe fed patch antenna, (b) Comparisons of E-plane coupled patch antennas on different permittivity and thickness substrate, magnitude of S11 and S21 vs. frequency when the distance between antennas is $0.5\lambda_0$ .....                  | 40 |
| Figure 4. 12. (a) H-plane coupled probe fed patch antenna, (b) Comparisons of H-plane coupled patch antennas on different permittivity and thickness substrate, magnitude of S11 and S21 vs. frequency when the distance between antennas is $0.5\lambda_0$ .....                 | 40 |
| Figure 4. 13. Mutual coupling reduction by EBG structures with different patch sizes: (a) geometry, (b) Magnitude of S21 obtained by FDTD simulation .....  | 41 |
| Figure 4. 14. Portable handset prototype with EBG ground plane .....  | 42 |
| Figure 4. 15. Artificial Magnetic Conductor (AMC) surface treatments (EBG structures) impede surface waves .....  | 43 |
| Figure 4. 16. Measured return loss and mutual coupling for the antennas shown in Figure 4. 15 .....   | 43 |
| Figure 4. 17. (a) Traditional power planes with connecting vias, (b) Power planes with EBG plate. The EBG plane is used to suppress the switching noise and noise induced from active devices or vias that passes through power planes ....                                       | 45 |
| Figure 4. 18. Top view of printed circuit board with a ribbon of EBG around it, this ribbon is used to suppress the radiation from PCB to provide shielding.....  | 45 |
| Figure 4. 19. (a) Two adjacent microstrip transmission lines on the perforated ground plane, (b) two intersecting microstrip lines on the perforated ground plane. Perforation, which resembles EBG structure, suppresses coupling interference and cross talk between lines..... | 46 |
| Figure 5. 1. Test Enclosure; box with Two EBG ribbons.....  | 48 |
| Figure 5. 2. (a) Schematic of connecting two cavity boxes to each other for an experiment, (b) Boxes covered with an EBG ribbon all around to investigate efficacy of EBG material for the interference coupling suppression.....   | 49 |
| Figure 5. 3. Dispersion Diagram of EBG pattern with $\epsilon_r = 2.2$ , $t = 1.54$ mm, $a = 4$ mm, $g = 0.4$ mm and cubic via with $d = 0.8$ mm (Pattern #1) .....   | 52 |
| Figure 5. 4. Dispersion Diagram of EBG pattern with $\epsilon_r = 4.8$ , $t = 1.54$ mm, $a = 4$ mm, $g = 0.4$ mm and cubic via with $d = 0.8$ mm (Pattern # 2) .....  | 52 |
| Figure 5. 5. shows the interference coupled inside the box from external source for two cases of with and without EBG patterns. Specification of EBG pattern #1 can be found in Table 5. I. ....  | 53 |
| Figure 5. 6. shows the interference coupled inside the box from external source for two cases of with/out EBG patterns. Specification of EBG pattern #2 can be found in Table 5. I.....   | 54 |
| Figure 5. 7. Air-filled rectangular CBS antenna fed with probe oriented in the y-direction. (a) Perspective view, (b) top view and (c) side view of (xy-plane)....  | 57 |

|  |    |
|--|----|
| Figure 5. 8. Geometry of two identical CBS antennas mounted on EBG ground plane (for antenna specification see Figure 5. 7), (a) top view (b) perspective view...  | 58 |
| Figure 5. 9. (a) and (b) show S-parameters of two identical CBS antennas mounted on a rectangular ground plane (blank case), for antenna specification see Figure 5. 7. Antennas can operate at 7.5 and 12.6 GHz as marked on plot. Also (b) shows coupling between antennas when EBG ground plane is used. Two different EBG designs for these two operating frequencies are implemented to show efficiency of these materials in coupling reduction, (for EBG structures specification see Table 5. II). S-parameters extracted by HFSS simulation. .... | 59 |
| Figure 5. 10. Dispersion Diagram of EBG pattern with $\epsilon_r = 4.8$ , $t = 1.54$ mm, $a = 4$ mm, $g = 0.4$ mm and cylindrical via with $d = 0.8$ mm (Pattern #1) .....   | 61 |
| Figure 5. 11. Dispersion Diagram of EBG pattern with $\epsilon_r = 3$ , $t = 1.54$ mm, $a = 2.6$ mm, $g = 0.4$ mm and cylindrical via with $d = 0.8$ mm (Pattern #2) .....   | 61 |
| Figure 5. 12. Total surface current density ( $J_{tot}$ ) (a) on the blank ground plane and (b) on the EBG ground plane when the CBS antenna is working at 7.5 GHz. The EBG pattern # 1 provides efficient gap at this frequency. For EBG structure specification see Table 5. II .....  | 63 |
| Figure 5. 13. Total surface current density $J_{tot}$ (a) on the blank ground plane and (b) on the EBG ground plane when the CBS antenna is working at 12.6 GHz. The EBG pattern # 2 provides efficient gap at this frequency. For EBG structure specification see Table 5. II .....   | 64 |
| Figure 5. 14. The antenna gain patterns at 7.5 GHz with/out EBG structures. The EBG pattern # 1 provides efficient gap at this frequency. For EBG structure specification see Table 5. II .....  | 65 |
| Figure 5. 15. The antenna gain patterns at 12.6 GHz with/out EBG structures. The EBG pattern # 2 provides efficient gap at this frequency. For EBG structure specification see Table 5. II .....   | 66 |
| Figure 5. 16. Propagation of wave in the free space and on the ground plane when CBS antenna is working at 7.5 GHz in two case of (a) blank and (b) EBG ground plane. The EBG pattern # 1 provides efficient gap at this frequency. For EBG structure specification see Table 5. II .....  | 68 |
| Figure 5. 17. Propagation of wave in the free space and on the ground plane when CBS antenna is working at 12.6 GHz in two case of (a) blank and (b) EBG ground plane. The EBG pattern # 2 provides efficient gap at this frequency. For EBG structure specification see Table 5. II .....   | 69 |
| Figure 5. 18. Two identical CBS antennas mounted on (a) Capacitive EBG ground plane, (b) Inductive EBG ground plane .....  | 71 |
| Figure 5. 19. Coupling Interference noise between two CBS antennas for three cases: I. Blank ground plane, II. Inductive EBG ground plane and III. Capacitive EBG ground plane. The CBS antenna is working at 7.5 GHz. The EBG pattern # 1 provides efficient gap at this frequency. For EBG structure specification see Table 5. II. For antenna specification see Figure 5. 7.....   | 71 |

## Chapter 1 : Introduction

Electromagnetic Interference (EMI) adversely affecting electronic devices is a critical challenge facing designers of electronic equipment operating at low threshold voltage levels. These challenges are intensified by an increase in system integration motivated by commercially-driven imperatives to increase functionality while reducing space and cost. EMI can be generated from or attributed to different hardware stages including the device, the chip, the package, the printed circuit board, interconnects and components, the chassis, and the peripherals. To minimize EMI, which could mean either reducing radiation from the equipment or increasing the immunity to external electromagnetic stimulus, various strategies are applied that are typically specific to each of these levels. It is important to note, that in addition to disrupting interference due to unintentional radiation, EMI is also of concern when using intentional radiators (i.e., antennas) that are placed in close proximity of each other, or that share common reference plane.

Electromagnetic noise or interference can be mitigated using one or more of several strategies. These strategies include, but are not limited to isolation of critical components, shielding, grounding, matching, filtering, addition of lossy materials and absorbers and finally the possibility of redesign of the circuitry of the victim device or the circuitry of the source of EMI. Eliminating the source of EMI is clearly desirable, but does not necessarily translate or equate to reduction in the susceptibility of the

device to external sources. In fact, strong interference can occur at frequencies different from the frequencies corresponding to the device switching speed, which makes the containment strategies even more challenging.

In this work, we focus on the generic problem of electromagnetic coupling between radiating (or receiving) devices positioned on a single chassis or positioned on separate chassis. Alternatively, and from a purely electromagnetic perspective, this set of problems can be described as coupling between antennas. However, this work will focus primarily on coupling through surface currents that is generated on the reference plane by the stimulus. Many problems fall under this category such as the problem of coupling between apertures (i.e., openings) present in the chassis or enclosure of an electronic device; the problem of coupling between two antennas sharing a common ground plane, radiated coupling between a distanced radiator and a cavity type antenna, coupling between internal devices within an enclosure to peripheral cables through ventilation holes or seams; external radiation through disk drive opening, etc.

According to literature implementing lossy material and absorbers has provided excellent shielding effect [1]-[4]. In previous works, lossy material and absorbers were applied to isolate interference between apertures or antennas sharing a common reference plane. However, while lossy materials have desirable electromagnetic features, mechanical and thermal properties can severely limit their applicability; additionally, cost can be an important factor as these materials need to

be engineered to work over specific frequency bands. Electromagnetic Band Gap (EBG) structures proposed over the past few years have inherent features that make them important in EMI/EMC applications [5]-[15]. This is primarily due to the fact that EBG structures suppress the propagation of surface waves over a specific frequency band that directly depends on the dimensions and type of the constitutive elements within the EBG structures [5]. Such feature was of secondary importance when these structures were originally conceived as the primary interest in these structures was the emulation of the naturally non-occurring perfectly magnetic conductor. This work focuses on the wave propagation suppression feature of EBG structures and proposes their use in practical EMI/EMC applications in the generic set of problems described above. Previous works investigated the effectiveness of EBG structures in suppression of unwanted electromagnetic energy in several applications. In [5]-[10], [21], [22], EBG structures were used to isolate antennas. In [11], [12], [14], [15], the EBG patches were used to suppress propagating waves within the power planes and parallel plates of printed circuit boards, thus dealing effectively with the problem of simultaneous switching noise and via coupling. EBG materials in [13] were used to suppress the radiation from Printed Circuit Boards (PCB), and they were used in [8] for signal integrity purpose.

In this work, we propose the application of EBG structures to the interior and/or exterior walls of enclosure to reduce coupling induced by surface currents. Such surface currents can be supported by either surface or traveling waves. We specifically focus on coupling between cavities which represent either openings in

chasses or antennas (i.e., radiating sources). Furthermore, we show that using different topologies in applying the same EBG structure provides different levels of interference suppression. Implementing EBG structures becomes more encouraging if newly introduced cascading method [23] is used. Cascading is a novel concept to ensure ultra-wide band gap. EBG structures will be designed to mitigate electromagnetic coupling within specific frequency bands. The design will be assisted by a commercial numerical code employing three-dimensional field solver. In this work, we have used the commercial full-wave Maxwell equation solver HFSS provided by Ansoft.

This thesis is organized as follow: in Chapter 2 we clarify the problems and challenges are faced by designers to provide EM immunity in electronics. In Chapter 3 several classical solutions for EMC purpose are reviewed. The EBG materials and their application for EMI reduction is presented in Chapter 4. In Chapter 5 we propose a new methodology for EM noise suppressions in cavities and enclosures and the summary of the work and critical need which directs the future work is given in Chapter 6.

## Chapter 2 : Problem and Challenges

Compliance to EMC standards is a great challenge for designers due to increasing amount of electromagnetic phenomena to which an electronic system should be immune. The performance of high-speed digital systems or integrated circuits is degraded by induced electromagnetic interference such as fast transient electrical pulses or bursts, electrostatic discharges, emissions from power or signal lines. To preserve the reliable performance of electronics, it is necessary to shield the electronics against the unwanted electromagnetic phenomena. Ever going increase in clock and bus speed in electronic circuits besides the continuous decrease in the threshold voltage levels of the components has intensified potential of degradation of performance through interference. Also today continuous advancement in the communication and electronics speeds up the need for complicated systems with several antennas or array of antennas and other electromagnetic sources in the same environment but, installing a new EM source (e.g., an antenna) because of possibility of mutual coupling interference between them is a challenging task. Mutual coupling degrades the performance of the EM source (e.g., an antenna) and it can cause undesirable effects such as side-lobes and blind angles. These unwanted EM interference is induced by radiation or conduction and it takes place in different levels including chassis, package, board, component and chip. Surface wave or current that propagates on metal surface is the support of major interference, which occurs in electronics. Surface currents radiates plane wave to space through scattering from



discontinuities and non-uniformities of metal surface. Then electromagnetic radiation directly or through surface waves interfere the operation of systems and components and degrades the reliable performance of the Electronics.

Isolation and minimizing interference and coupling noise methodologies have been evolved in the course of progress and advancement of electronics circuits. One of the primarily addressed problems in this context was noise reduction in low frequency electronic circuits. Many circuit designers suggested using de-coupling capacitors to introduce low pass filters that remove high frequency transients on power supplies and noise induced on the leads and wires in the circuits. Today, increase in operational frequency of the electronic processors has imposed the need of having dedicated methods for different levels of electronic circuits. For instance, it is necessary that interfered noise on power plane of an electronic board is suppressed locally, before it is propagated to the other parts of the circuit. Also, the increasing demand to reduce the size of electronic circuits requires techniques to mitigate coupling interference between closely located transmission lines and electronic components in a dense integrated circuit. Noise reduction in interconnects is a key issue. Additionally, minimizing of EM radiation from printed circuit boards and shielding provided by enclosures considering the resonance frequencies of the packages, apertures and openings are among the highly used methods to achieve EMC required by standards. Also it is required that EM sources like antennas are isolated from interference of other external EM sources. Therefore, research on EMI

reduction methodologies is highly motivated by the industry needs as the electronic circuits become more complicated and dense.

Now we focus on the EMI in package level. For EMC purpose a shielding metallic enclosure typically used to attenuates emissions from electronic equipments. However slots and openings, such as those due to windows and displays, or those for cooling purpose and ventilation, cable and port connections, CD-ROM's and disc-drivers and speakers degrades shielding effectiveness of enclosures. As a result coupling of energy between internal and external electromagnetic sources in package and cavities through aperture and openings and coupling of energy through reflected or radiated field from surface of shield become considerable concern for EMC. Also shielding much more is degraded if the wavelengths of fundamental frequency of interference source or its harmonics are in the order of slot apertures length or if the intrinsic resonance of the enclosure, which produce intense internal field, is excited by this interfering signal. Therefore it is necessary to understand coupling mechanism to provide reliable shield for electronic systems.

Following in the next chapter the solutions proposed to suppress the interference noise are reviewed.

## Chapter 3 : Classical Solutions

The EM interference noise degrades the reliable performance of the system. Interference takes place in different levels including chassis, package, board, component and chip. The mechanism of this interference is due to the radiation or conduction. To meet EM Compatibility and reduce EM noise various strategies are applied in these levels. These strategies include: separation, shielding, grounding, matching, filtering, change in orientation, implementing lossy materials and absorbers and finally electronic redesign of the victim device or the source of EMI. In continue the efficiency of the different methods of interference suppression on two different scenarios is presented. First we consider an enclosure and then we look at cavity backed slot antenna.

### 3.1. *Electromagnetic Interference Reduction in Packages and Enclosures*

To reduce EM interference noise a shielding metallic enclosure typically used to attenuates emissions from electronic equipments. However slots and openings, such as those due to windows and displays, or those for cooling purpose and ventilation, cable and port connections, CD-ROMs, disc-drivers and speakers degrades shielding effectiveness of enclosures. Therefore coupling of energy between internal and external electromagnetic sources in package and cavities through these

openings and coupling of energy through reflected or radiated field from surface of shield become considerable concern for EMC. Also if the wavelengths of fundamental frequency of interference source or its harmonics are in the order of slot apertures length, shielding much more is degraded. Similar scenario happens if the intrinsic resonance of the enclosure, which produce intense internal field, is excited by this interfering signal. Following a few classical strategies to suppress coupling interference in package level are addressed.

#### 3.1.1. Change in configuration of openings

The size and shape of the openings on enclosure affect the electromagnetic coupling [16], [17]. The studies on different configurations mainly have cleared the mechanism of interference coupling, relation between EMI and aperture length and also how multiple slots and openings interact on each other. Wang et al. [16] has considered different scenarios for comparison purpose. The problem they studied was consisting of an empty shielding metallic enclosure and apertures in front sides of the enclosure. The enclosure was illuminated by Gaussian transit plane wave which emitting normally to openings. The viewpoint was located in center of box to collect the data.

That experiments and investigation showed that the first resonance of thin slot is typically half-wavelength resonance, so it is necessary to choose the slot length in a way not to excite the resonance of enclosure or not the same as operational frequency

of electronic system. When the slot width increases it is allowed for penetration of more electromagnetic energy so we have more strong interference but on the other side wider slot cause the amplitude of the electric field produced by slot resonance to decrease. Also studies showed resonant behavior of apertures with different geometry inside the enclosure are almost same if the areas of the openings remain same. If it is necessary to have several parallel slot and opening on enclosure wall it is better to make all the slots and openings same length to prevent additional resonance. In this scenario resonant dominated by thinnest slot while energy of EMI mainly declared by wider slot. As the number of similar slot close to each other increases, the amplitude of the resonance decreases significantly. Therefore, for heat dissipation and air ventilation it is advisable to have an array of fine apertures like honeycomb to make the EMI penetration as small as possible.

### 3.1.2. Implementing Lossy Material to Enclosures and Openings

The leakage of electromagnetic wave through apertures and opening is critical in the frequencies near to the resonance frequencies of the aperture and the enclosure. Implementing lossy material and absorbers around the aperture or inside the enclosure is an effective technique, which suppress the radiation significantly. By using this technique there is no need to design the size of enclosure box or size and number of apertures on enclosure used to shield the electronic system. The lossy materials are implemented inside the package to lower the Q of the box [18], [19]. This method decreases possibility of radiation because of the resonance of the box.

The advantage of using coating around the aperture [2], [4], [20] is that it can be used easily without need to change the topology of apertures on package. Applying lossy materials, which are available in market, can provide significant attenuation on resonance of the aperture and the box. But heat and mechanical resistibility of these materials are on concern. These materials change the electromagnetic power of the interfere wave to the thermal power. They are typically fragile materials that need mechanical support to be implemented around apertures or they can be implemented on conductor around the aperture. However because of specifications mentioned, the lifetime of these materials is limited. Already research for providing materials with better properties is continuing.

### 3.1.3. Design of Package according to PCB features

In this method an enclosure is designed with the specific dimensions to have opportunity of the positioning electronic circuits inside the package in a way to reduce the power loss due to resonant modes of the package [19]. After designing of an electronic circuit, features of PCB in regards to location of high voltage and current on the board are investigated. Then a package is designed to have capability of positioning PCB inside it considering that intense E-field on the board is located in low H-field in the box and vice versa.

### 3.2. Electromagnetic Interference Reduction in Cavity Backed Slot Antennas

Cavity Backed Slot (CBS) antennas are resonant cavities, which radiates through aperture and slit to the free space. CBS antenna has broad range of applications in space vehicles, satellites, radar and mobile telephony as they are easy to manufacture, small in size, light weight and they can be mounted on the surface of the vehicle without affecting its aerodynamics. CBS antennas and coupling between two antennas have been analyzed in numerous papers [1], [24]-[26]. CBS antenna according to desired operating frequency is designed similar to a resonator. For instance the CBS antenna, which considered by Omiya et al. [24] is showed in the Figure 3. 1. The cavity is chosen under the assumption which  $TE_{101}$  mode is excited. This antenna is working at 2.45GHz. A quarter of wavelength probe (29.5 mm) is used to excite the cavity. The separation between the slot and probe is half wavelength (61.5 mm). The operating frequency of CBS antenna can be extracted from  $S_{11}$ . The return loss plot measured and computed by FDTD method by using hanning window in that work and it is showed in Figure 3. 2.

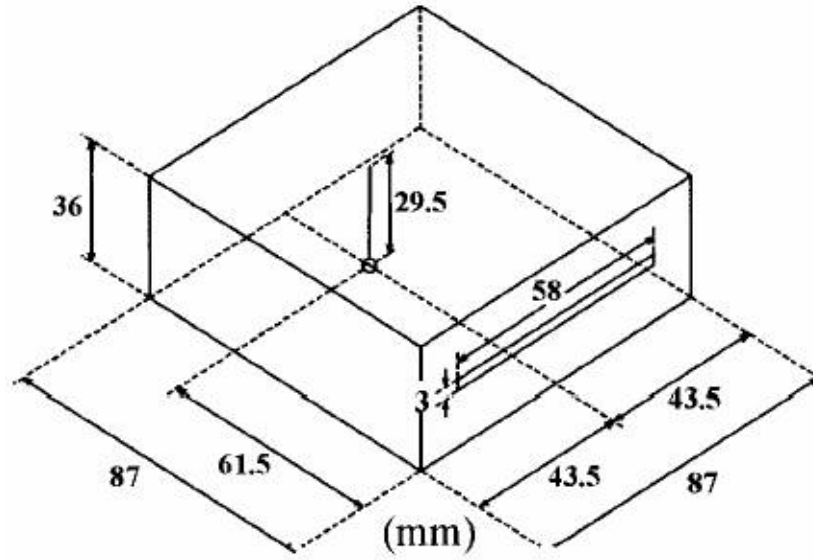


Figure 3. 1. Geometry of the cavity-backed slot antenna<sup>1</sup>

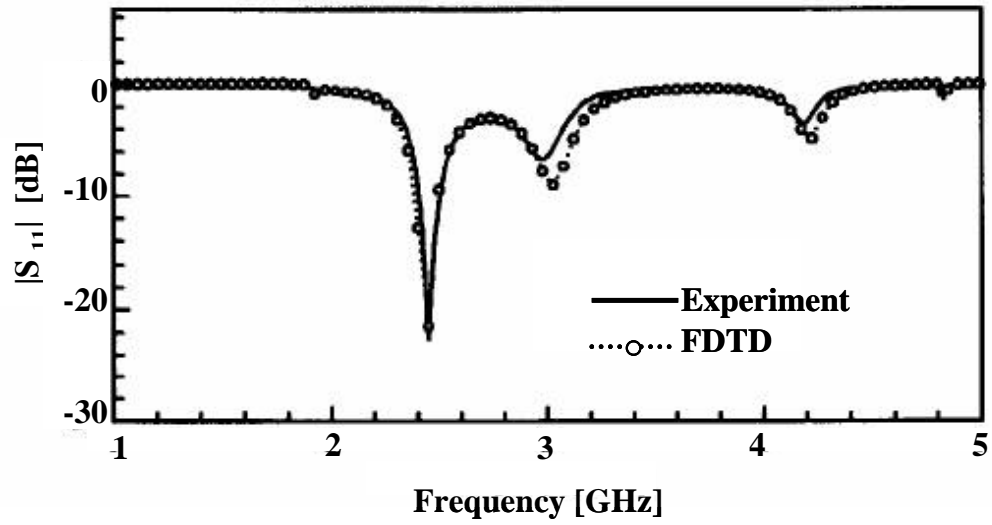


Figure 3. 2. Return loss of CBS antenna specified in Figure 3. 1 by measurement and FDTD simulation<sup>2</sup>

<sup>1,2</sup> These figures have been taken from ref. [24]



While continuous advancement in communication and electronics speeds up the need for complicated systems with several antennas or arrays of antennas in the same environment but installing a new antenna because of possibility of mutual coupling interference between them is a challenging task. Mutual coupling degrades the performance of an antenna by causing undesirable effects such as side-lobes and blind angles. The coupling reduction techniques including incorporation of lossy substrates, ground plane slits, slot antenna E-plane and H-plane configurations and separation distance between antennas have been presented for CBS antennas by Georgakopoulos et al. [1]. Following we review these different methodologies and results presented in [1] for suppressing interference coupling.

A 3-D view and geometry of CBS antenna is used in the above study is exhibited in Figure 3. 3. In simulation two CBS antennas mounted on the finite ground plane of dimension 10x6 cm. Figure 3. 4 shows the geometry of two identical CBS antennas on a ground plane.  $S_{12}$  shows coupling between two antennas. Coupling between antennas when antennas connected to each other without existence of extra materials or structures labeled “blank” for reference purposes. As it is clear from  $S_{11}$  graph in Figure 3. 5, this specified CBS antenna could work at 7.5GHz and 11.92 GHz.

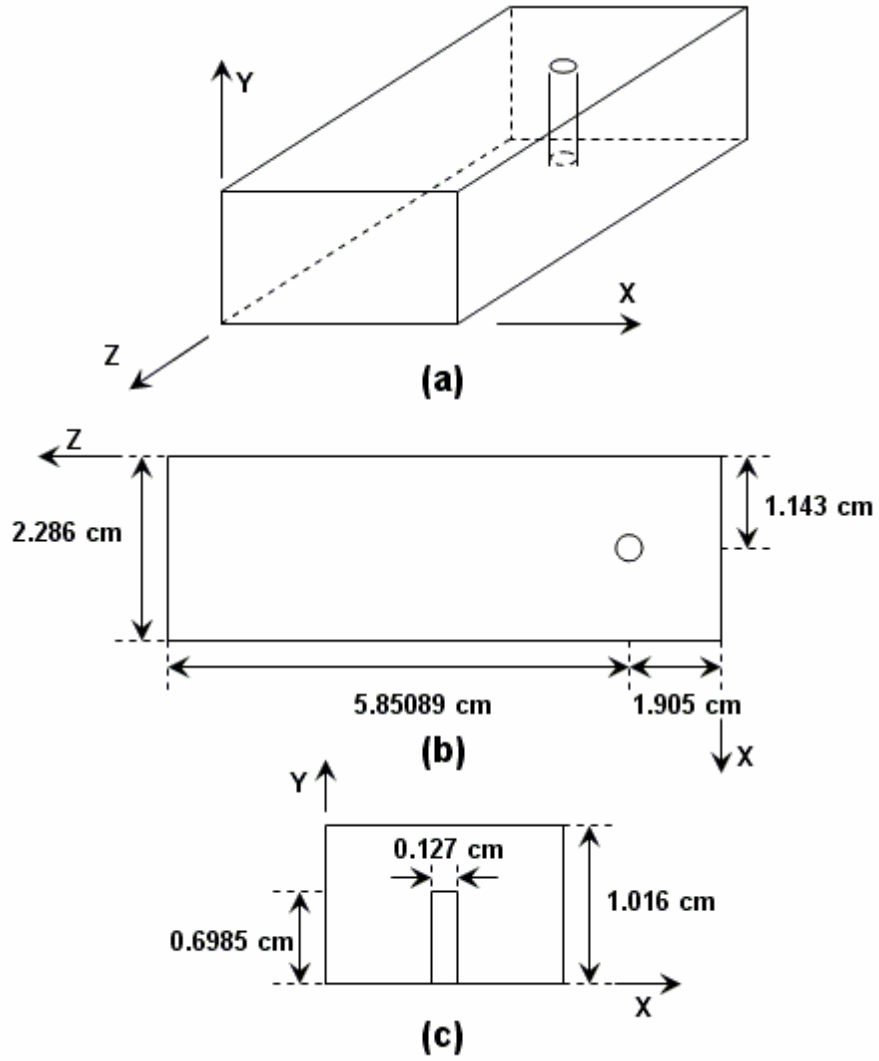
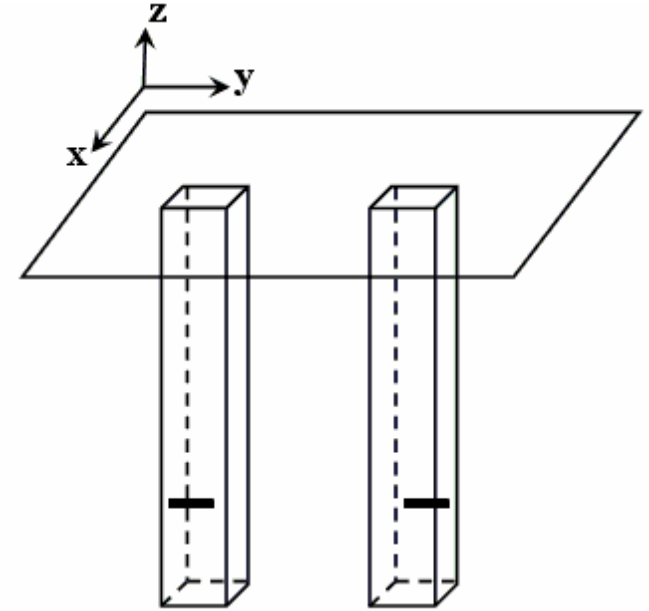
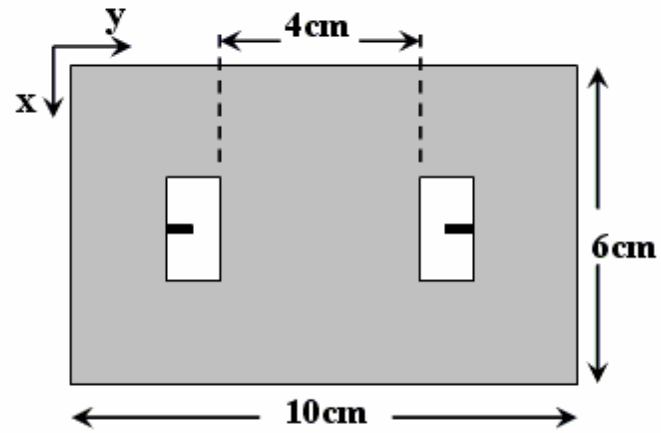


Figure 3. 3. Air-filled rectangular CBS antenna fed with probe oriented in the y-direction.

(a) Perspective view, (b) top view and (c) side view of antenna



(a)



(b)

Figure 3. 4. Geometry of two identical CBS antennas mounted on rectangular ground plane (for antenna specification see Figure 3. 3), (a) perspective view and (b) top view

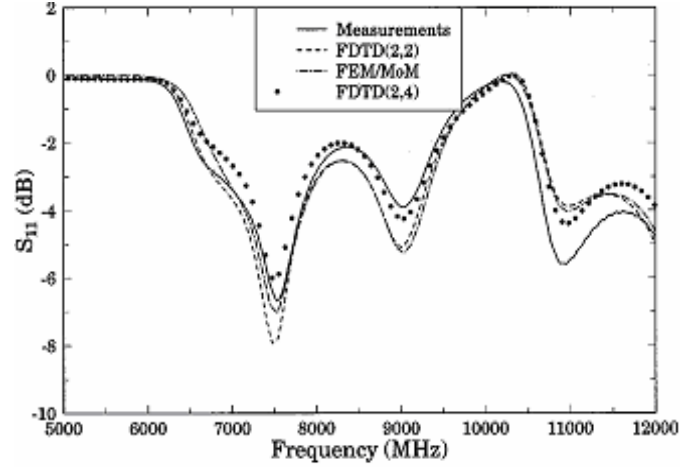


Figure 3. 5 Magnitude of S11 of two identical CBS antennas mounted on a ground plane. These data extracted by measurement and numerical analysis (The numbers in front of FDTD method show order of accuracy in time and space domains). For antenna specification see Figure 3. 3<sup>1</sup>

### 3.2.1. Implementing Lossy Materials

The lossy material attenuates EM wave so it can be a good choice for suppressing interference in EM system. Studies showed if the same lossy material with different thickness fills space between two antennas (Figure 3. 6), the thickest one can mitigate coupling more efficiently. The effect of ECCOSOB GDS electric/magnetic composite material of 1.5 mm, 3.0 mm and 4.5 mm were studied on coupling interference. The average spec of this material is:  $\epsilon_r = 13.4$ ,  $\sigma = 0.17 \text{ S/m}$ ,  $\mu_r = 1.5$  and  $\sigma^* = 95000 \text{ } \Omega / \text{m}$ , where  $\sigma$  and  $\sigma^*$  are the electrical and magnetic conductivities respectively.

<sup>1</sup> This figure has been taken from ref. [1]

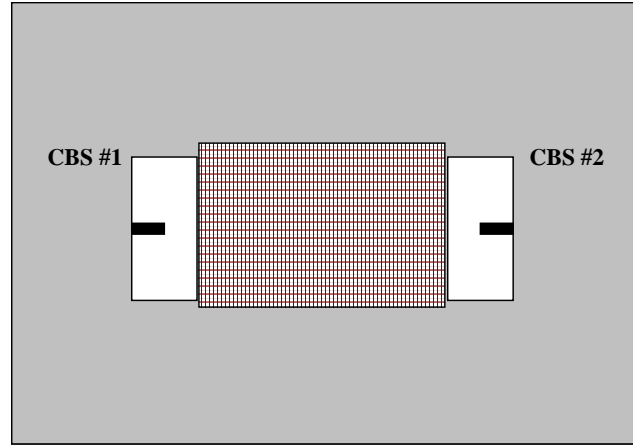


Figure 3. 6. Top view of CBS antennas on a ground plane with GDS superstrate in between

Figure 3. 7 shows results of coupling gained by simulation and measurement. For the 1.5 mm thick GDS coupling reduced maximum 4 dB, for the 3.0 mm thick maximum reduction is 6 dB and for the 4.5 mm thick maximum reduction is 7 dB. The maximum coupling is defined as maximum over entire band of frequency. The reduction of coupling in lossy material is mainly related to the minimization of surface current on ground plane.

### 3.2.2.Slit on the Ground Plane

In this method coupling interference is reduced by introducing discontinuity such as slit on the route of surface current on the ground (Figure 3. 8). To investigate the effect of discontinuity a 2 mm, 4mm and 8 mm slit was symmetrically cut at the

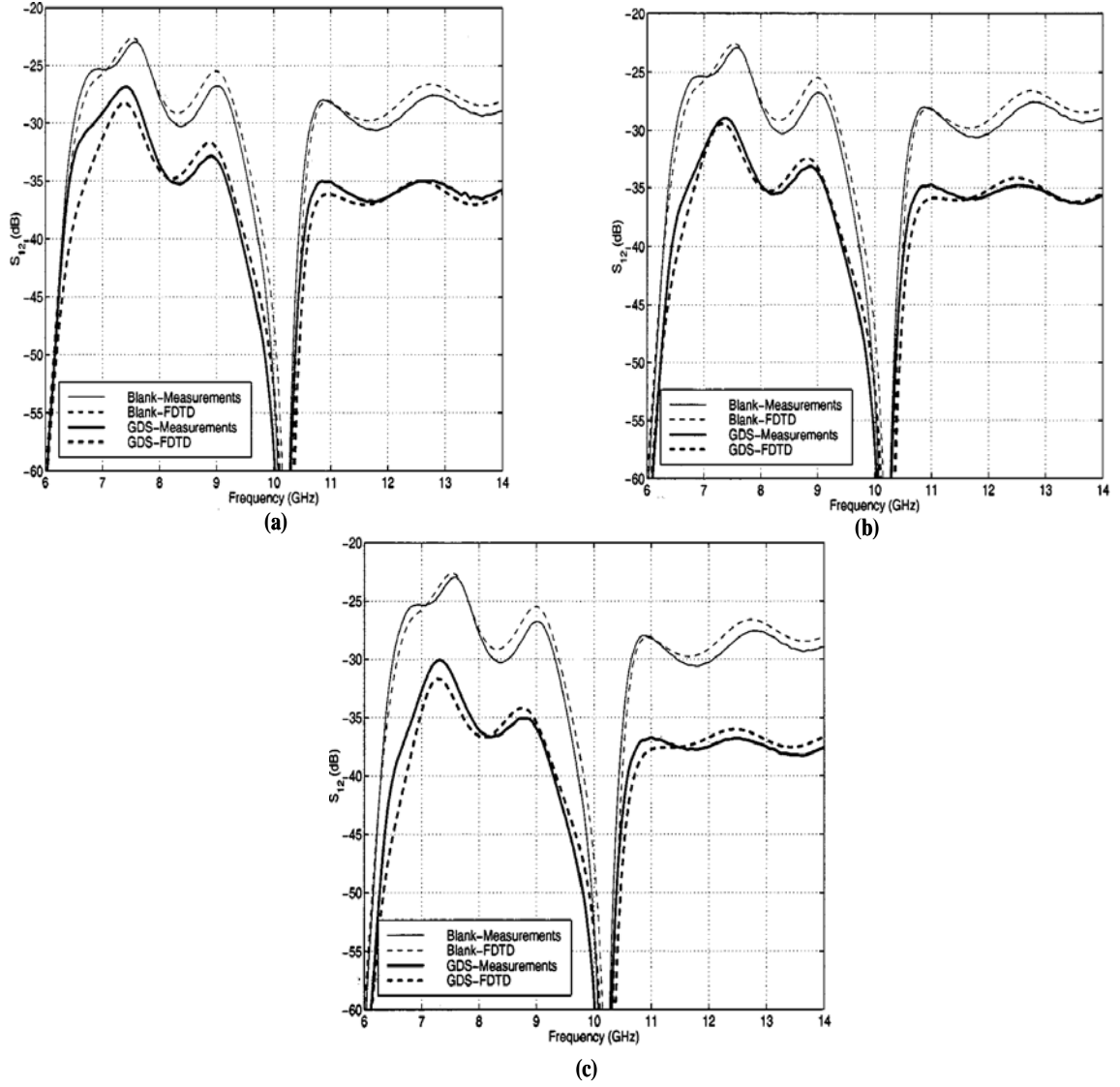


Figure 3. 7. Both measured and simulated coupling interference between two CBS antennas with and without presence of lossy superstrate in three cases of (a) 1.5 mm thick GDS, (b) 3.0mm thick GDS, (c) 4.5 mm thick GDS<sup>1</sup>

<sup>1</sup> This figure has been taken from ref. [1]

center of ground plane. Figure 3. 9 shows the results. It is seen that coupling reduction doesn't change dramatically when the width of the slit becomes bigger compare to 2 mm slit at frequencies around 7.5 GHz. But at higher frequencies around 11.92 GHz the coupling reduction is larger when the slit is wider. The slit is electrically larger at higher frequencies, thereby the surface current disrupted on the ground.

Implementing lossy material much preferable than cutting slit on the ground, as mechanical strength of the ground plane isn't affected in the former. In addition GDS provides more attenuation in coupling interference.

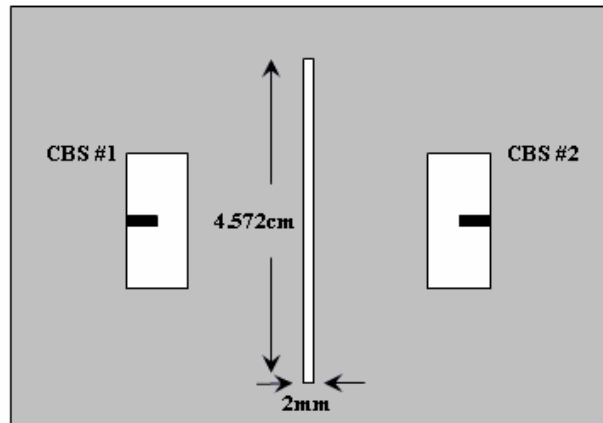


Figure 3. 8. Ground plane with slit to reduce mutual coupling between antennas<sup>1</sup>

---

<sup>1</sup> This figure has been taken from ref. [1]

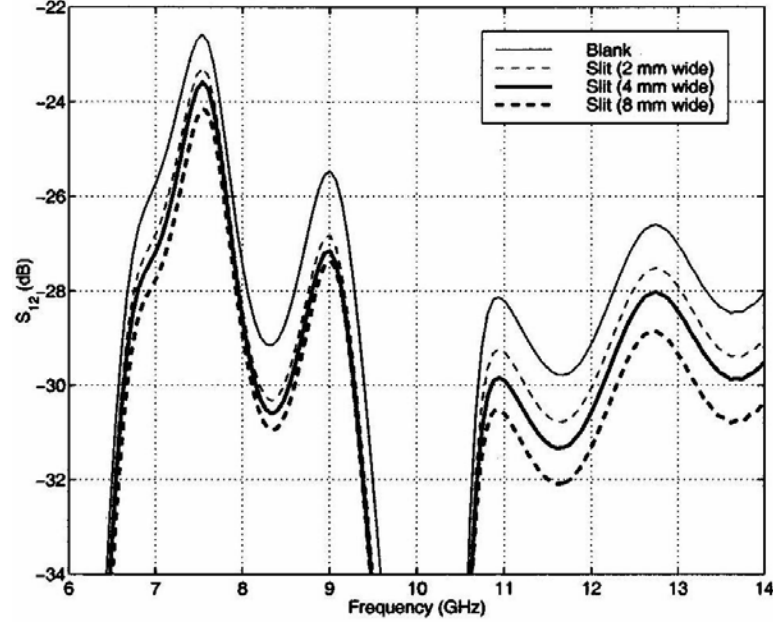


Figure 3. 9. Coupling with a different slits on the ground plane<sup>1</sup>

### 3.2.3. Change in Configuration

Change in orientation of antennas affects the mutual coupling between them. As it is shown in literature [30], [1], in side-by-side antennas the E-plane configuration exhibits the smallest coupling for electrically small separation distances and H-plane configuration exhibits the smallest coupling for electrically large separation distances. Figure 3. 10 shows E-plane versus H-plane configuration. In the CBS scenario mutual coupling between antennas is less intense when they are oriented in H-plane (Figure 3. 11). In this configuration antennas have placed in the direction of minimum radiation.

<sup>1</sup> This figure has been taken from ref. [1]



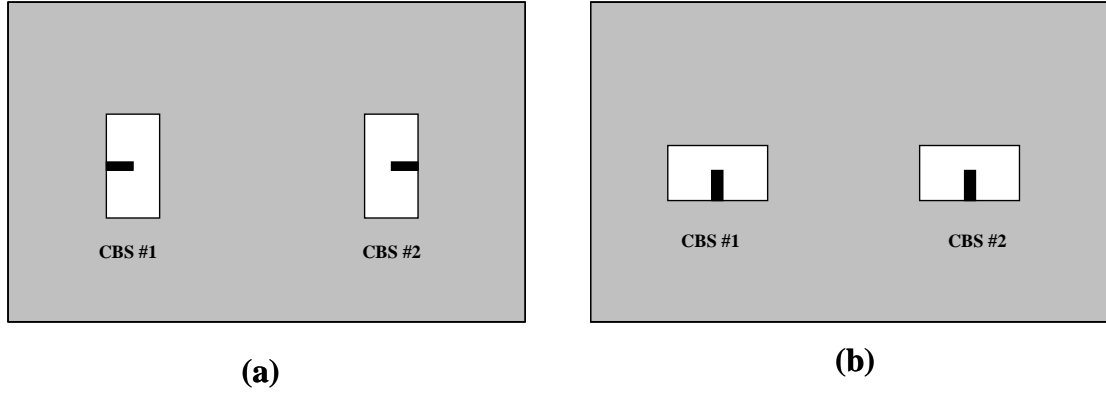


Figure 3. 10. Top view of two CBS antennas with (a) E-plane and (b) H-plane configuration

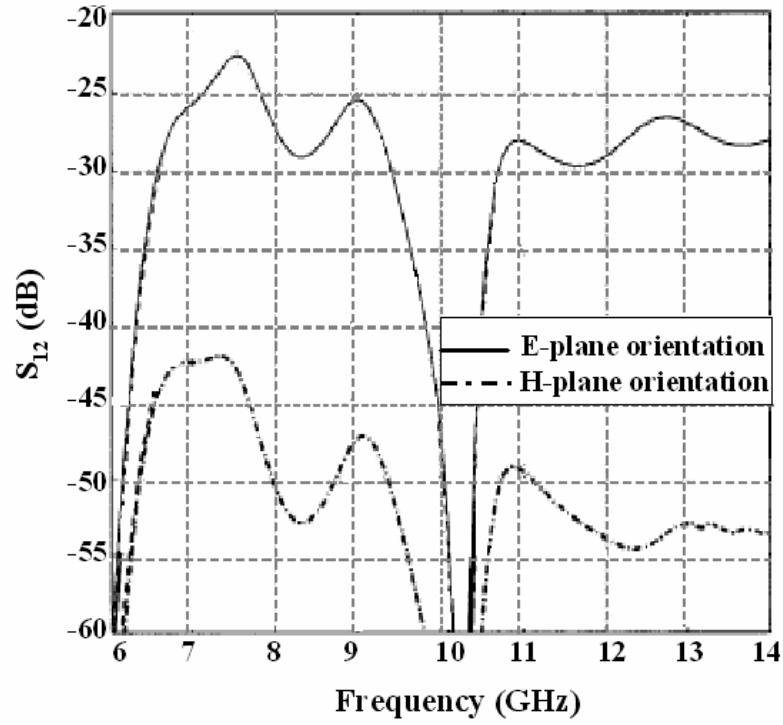


Figure 3. 11. Coupling between two CBS antennas oriented in different directions<sup>1</sup>

<sup>1</sup> This figure has been taken from ref. [1]

### 3.2.4. Separation Distance

Obviously coupling decreases as the separation between the two antennas becomes larger. Figure 3. 12 shows coupling between two CBS antennas by changing separation distance between them.

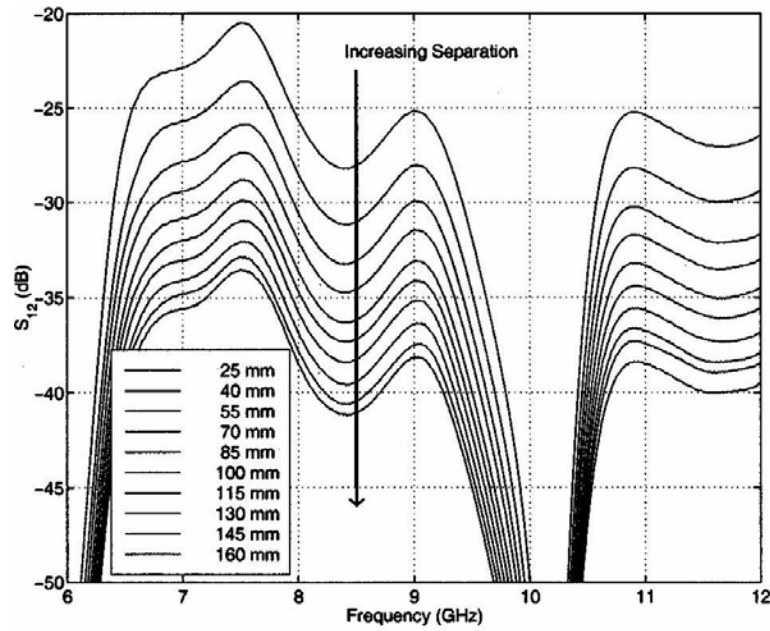


Figure 3. 12. Coupling between two CBS antennas for different separation distances<sup>1</sup>

<sup>1</sup> This figure has been taken from ref. [1]

## Chapter 4 : Electromagnetic Band Gap (EBG) Materials

### *4.1. EBG Structures*

EBG structures operating in the high frequency and the microwave frequency bands are periodic or quasi-periodic patterns created by inclusions in dielectric or magnetic material [5], [27], [28]. The EBG structures are also referred to as high-impedance surfaces, metallo-dielectric material, negative materials, and possibly other designations. In this study, we use the simplest form of EBG patterns represented generically by the schematic shown in Figure 4. 1. These structures are characterized by periodic metallic patches connected to a common ground (or reference) plane by short stubs or plated through-holes (commonly referred to as *vias*). The material between the patches and the ground plane can be dielectric or magnetic material, or a combination of the two. In this work we consider square patches. This choice does not diminish the generality of our work as other topologies of similar size are applicable with similar effects. The critical parameters of the EBG patches are illustrated in Figure 4. 1. These include the patch size, gap or distance between adjacent patches, diameter of stubs, height and material of the substrate. The geometrical features of the patches directly relate to the frequency of the stop band.

A major property of the EBG is the suppression of EM waves as originally postulated and experimentally demonstrated by the ground breaking work of Sievenpiper et al. [5], [28]. This fundamental property of HIS structures positions them to play a highly critical role in the field of EMI/EMC and signal integrity. To

provide better view for this property we look at the  $S_{\text{paramets}}$  between two ports inside the parallel plates. These plates filled with EBGs which is made of FR4 dielectric, 4 mm square patches and vias with .4 mm radius and 1.54 mm height. The stop band of this EBG structure is showed in Figure 4. 2.(a). If we look at the Electric field inside the parallel plates in Figure 4. 2.(b) and surface current on the plate in Figure 4. 2.(c) at 6.6 GHz (inside the stop band) we can see that these structures can suppress the propagation of waves. Another interesting property that already has attracted these structures in many antenna applications is existence of non-destructive phase reversal in relevant band gap from EBG textured reflector sheet

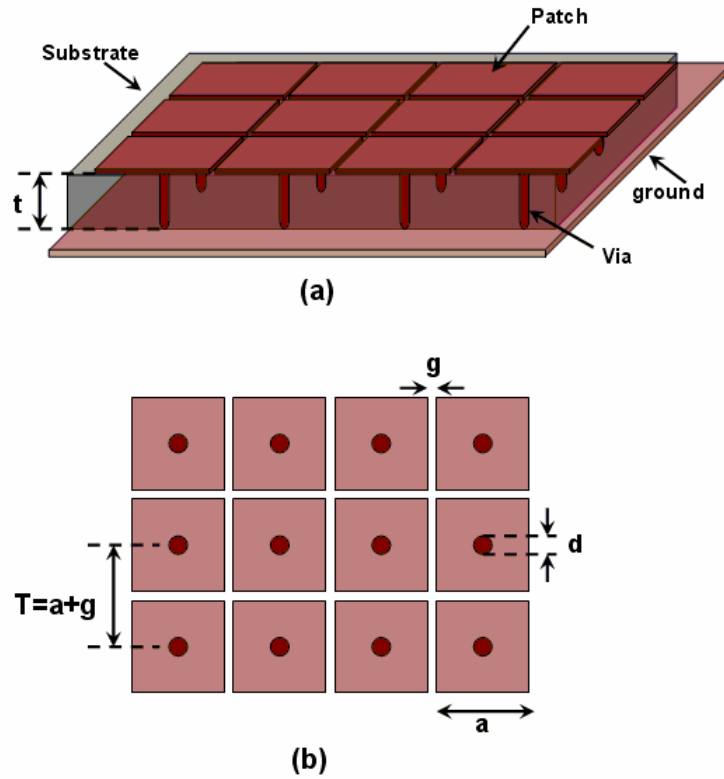
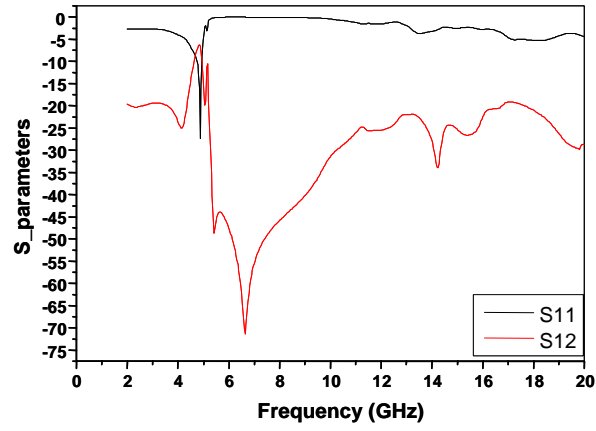
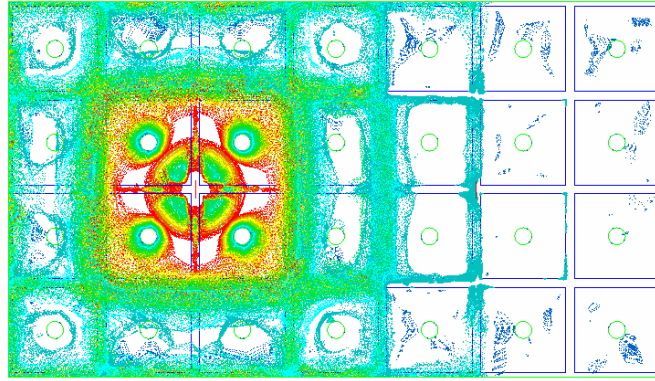


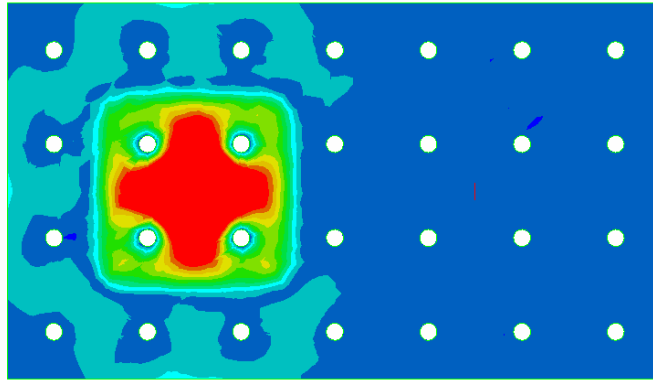
Figure 4. 1. Geometry of EBG Ground plane (a) perspective view (b) top view



(a)



(b)



(c)

Figure 4. 2.(a)  $S_{\text{parameters}}$  between two ports inside the parallel plates filled with EBG structures, (b) magnitude of electric field inside the parallel plates at 6.6 GHz, (c) surface current on the plate at 6.6 GHz

in normal incidence. These properties have opened several research areas including: (1) finding out different designs in small sizes with wider band gaps, (2) finding out closed form formulas, which relate the structures dimension and properties to band gap specification and (3) finding out new applications in applicable electromagnetic areas.

In the following sections we are going to review different studies which used EBG structures as stop band filters to suppress interfering EM signal. Also we will propose novel method of using EBG structure that eliminates interfering surface currents arising from other on-chassis radiators and also surface currents induced on the device enclosure arising from distanced radiating objects. The basic idea is to encircle the object that needs to be protected (antenna, aperture, device ...etc.) with a ribbon of HIS structure that is carefully designed around the frequency of interest. In effect, the HIS structure acts as a medium with either negative  $\mu_r$  or negative  $\epsilon_r$ , occurring within a specific frequency band. By changing the texture of surface conductor to EBG patterns, the frequency property of the surface is changed. These designs provide high impedance boundary condition against the propagation of surface wave, which in ideal case it can be described as Perfect Magnetic Conductor (PMC). In the gap the tangential magnetic field is very small and electric field is very big. The HIS structure can be viewed as a plasma medium resonating over a band of frequencies. While plasma media have been available for many years, the EBG structure offers the strong band stop characteristics of a plasma medium that can be produced inexpensively using printed circuit board technology.

#### 4.2. Design of EBG Structures

There are a few primary closed form formulas for describing property of these periodic structures using lumped elements model when the structure is small enough comparing to wavelength. The parallel LC resonator which acts like a band stop filter is one of them showed in Figure 4. 3. To the best of our knowledge there is no exact or even reasonably accurate closed formula that relates the geometrical parameters of the EBGs to the frequency of band stop. Therefore, and until a highly accurate closed-form expression is developed, the effective band of an EBG structure needs to be generated directly or indirectly using numerical simulation tools. When using numerical codes to extract the effective band of these structures, several techniques can be used with varying complexity and efficiency. Two methods commonly used

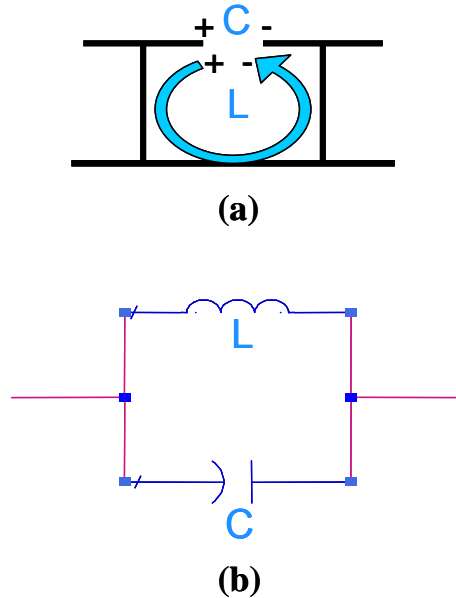


Figure 4. 3 (a) Side view of EBG structure, (b) Equivalent circuit model of (a)

are extracting the S-parameters between two ports placed across the EBG structures, which is a direct method in the sense of giving  $S_{12}$ . A second numerical procedure is extracting dispersion diagram, which is indirect method in the sense that it is obtained first and then implemented in the defined application to obtain  $S_{12}$  between two ports. Following we explain these methods in more details.

#### 4.2.1. Scattering parameters

Scattering parameters or S-parameters can be used to analyze the performance or extract specification of these structures. This methodology is easy and it can be obtained through measuring of transferred and reflected power between two ports placed across the EBG structure as shown in Figure 4. 4. If this method is used to design EBG structure with specific band stop it is a trial and error procedure and is the most direct. It is direct because at the same time when it gives the location of the band gap, its width and its center, it provides the level of signal attenuation at different frequencies too.

Figure 4. 5.(a) shows the magnitude of  $S_{12}$  of a parallel plate waveguide loaded with designed EBG. As it is clear for that design the gap is located almost from 2 to 4 GHz. For comparison purpose the dispersion diagram of this EBG structure is presented in Figure 4. 5.(b).



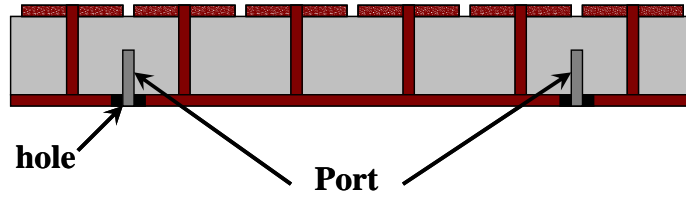
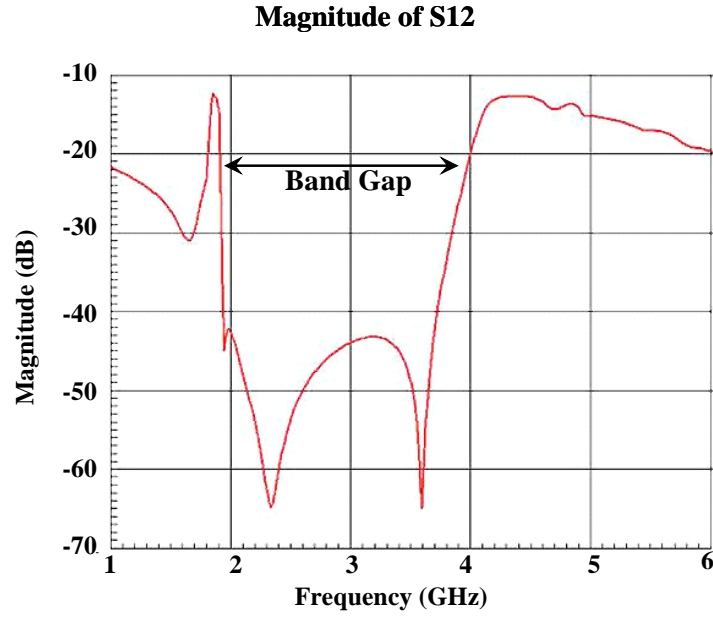


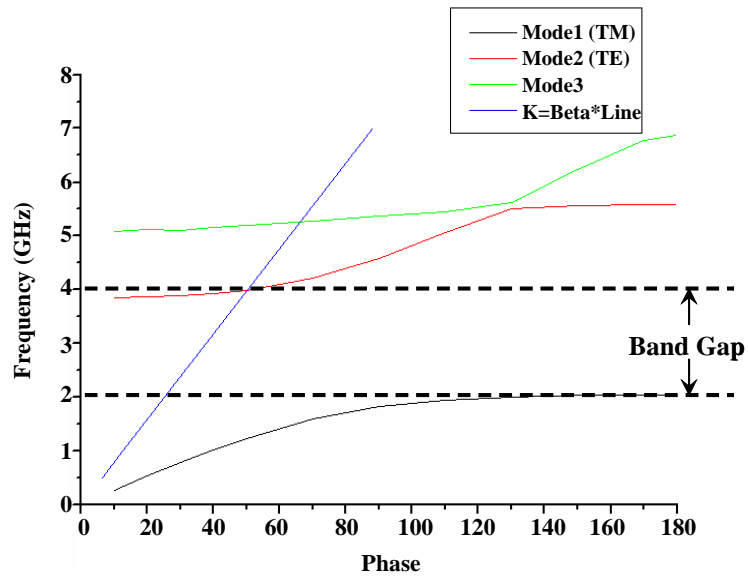
Figure 4. 4. A setup for extracting band gap of EBG structures using S-parameters, coupled field between ports (i.e. SMA connectors) which positioned across the EBG structures illustrates band stop

#### 4.2.2. Dispersion Diagram

The dispersion diagram or  $(\beta-\omega)$  diagram or  $(k-\omega)$  diagram is extracted by considering only one patch (or a unit cell) and applying a periodic boundary condition on the sides of the cell (to mimic a periodic structure extending to infinity) and PML boundary condition on the top open wall as shown in Figure 4. 6. Irredundant data from analysis of unit cell on Brillouin [29] Zone which shows irreducible triangle considering periodicity and symmetry can be extracted. Phase which shows wave vector as a variable is changed between linked boundaries on sides of BZ triangle. Eigensolution for this variable illustrates frequency in which wave propagates. In other words, dispersion diagram shows relationship between wave vector and frequency. This diagram presents propagating modes and band gaps possibly exist between modes. In this work we used HFSS simulation tool to solve Maxwell's equation on a cell. Figure 4. 7 shows the top view of a unit cell. The dimensions of periodic structure are clear in this figure.



(a)



(b)

Figure 4. 5.(a) Magnitude of  $S_{12}$  and (b) Dispersion Diagram of parallel plate waveguide loaded by EBG structure. Specification of EBG is: patch of 10 x 10 mm, gap of .4 mm, via with radius of .4 mm, substrate with  $\epsilon_r = 4.4$  and height of 1.54 mm

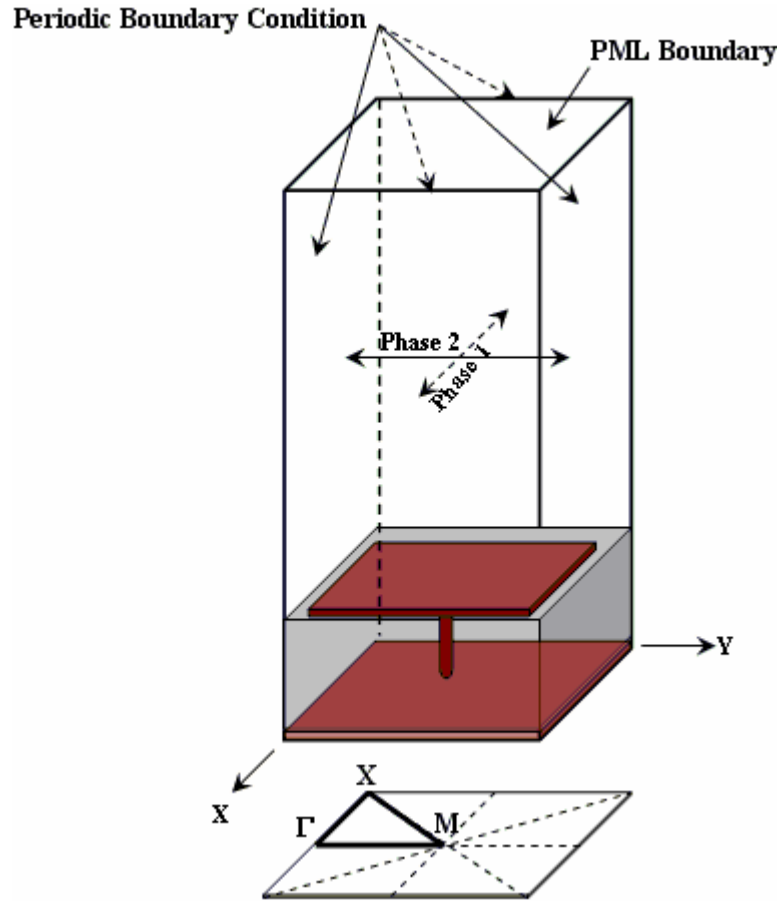


Figure 4. 6. shows a unit cell of EBG material and the boundary setting. Also Brillouin triangle is displayed in this figure. Using this setup we extract dispersion diagram which is used to specify band gap

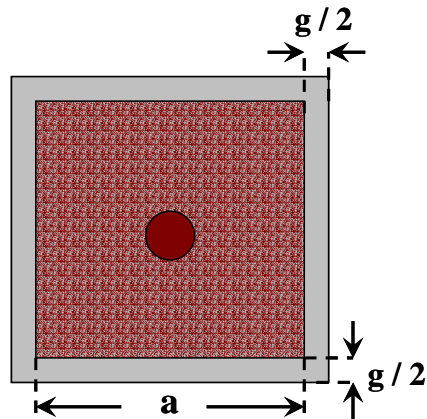


Figure 4. 7. Top view of a unit cell of EBG structure with periodic square patch of length  $a$  and gap length of  $g$

The calculation of dispersion diagram on the sides of BZ triangle involves three steps. First, in the X- $\Gamma$  direction the phase difference showed by *phase 2* is fixed to 0 between two parallel sides of a unit cell and phase difference between two other sides showed by *phase 1* is varied from 0 to 180 degrees. Then Maxwell's equations are solved for each phase relation to calculate the permissible eignsolutions. This step shows one-dimensional propagation. In the second step, in the  $\Gamma$ -M direction *phase 1* is fixed on 180 degrees and *phase 2* is varied from 0 to 180 degrees and similarly Maxwell's equations are solved. Also this step shows one-dimensional propagation. In the third step, in the M-X direction, both phase differences between parallel sides of unit cell are changed simultaneously from 180 to 0 degrees which corresponds to the two dimensional propagation.

For instance the dispersion diagram of one of the EBG structures which is used in this work is shown in Figure 4. 8. A band gap can be seen between two modes (not necessarily between first and second modes). In the dispersion diagram the free space frequency-wave vector line shows the free space speed limit. Therefore the gap between upper limit of TM mode and intersection of this line with TE mode shows forbidden region, irrespective of the direction of propagation and polarization.

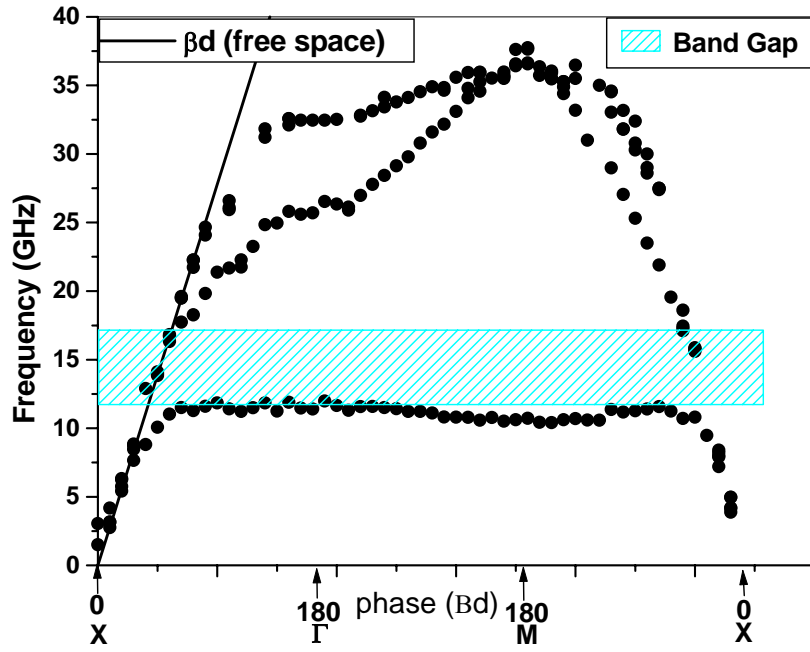


Figure 4. 8. Dispersion diagram of an EBG structure, in this structure the band stop is extended from 11.9 to 17.3 GHz

#### 4.3. Surface Wave

Surface waves can exist on the interface of dissimilar materials with non-positive permittivity or permeability such as metal [5]. They are bound to the interface and decay exponentially into surrounding materials. At microwave frequencies associated fields can extend thousands of wavelengths into surrounding space and therefore these waves also described as surface currents. They can be modeled effectively by surface impedance.

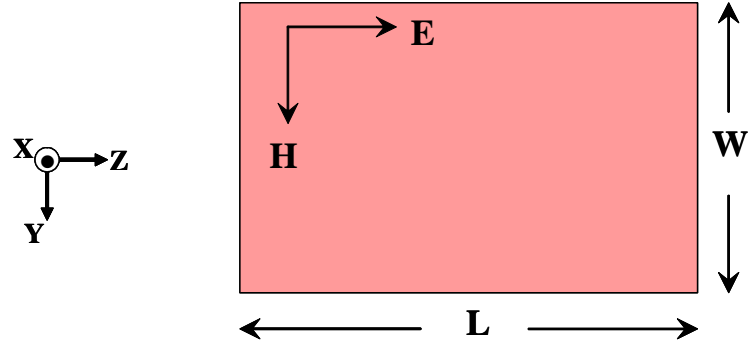


Figure 4. 9. A rectangular surface for computing impedance surface

As already it is known surface current can occur on the interface of metal and free space. By applying textures to the metal surface, we can change the surface impedance or surface wave properties. Following we extract impedance for a surface of width  $W$  and length  $L$  (Figure 4. 9). The voltage across the length of surface is given by:

$$V = E_z \cdot L$$

Equation 4. 1

The current on the surface is equal to:

$$I = H_y \cdot W$$

Equation 4. 2

The surface impedance is defined by ratio of electric field over magnetic field at the surface:

$$Z_s = \frac{E_z}{H_y} = \frac{V}{I} \left( \frac{W}{L} \right)$$

Equation 4. 3

The impedance surface which show surface wave properties can be derived as following. Assuming the surface is in YZ plane and the surface wave propagates in the +Z direction and field decays in the +X direction (the geometry of problem is shown in Figure 4. 10), the electric TM field can be written in this form:

$$E_z = A \cdot e^{-jkz - \alpha x}$$

Equation 4. 4

$H_y$  can be derived from the Ampere's law ( $\nabla \times H = \varepsilon \frac{\partial E}{\partial t}$ ):

$$j\omega\varepsilon E_z = \frac{\partial H_y}{\partial x}$$

Equation 4. 5

Solving Equation 4. 5 using Equation 4. 4 gives:

$$H_y = \frac{-j\omega\varepsilon}{\alpha} A \cdot e^{-jkz - \alpha x}$$

Equation 4. 6

Inserting Equation 4. 4 and Equation 4. 6 in Equation 4. 3 surface impedance for TM surface wave is gained:

$$Z_s(TM) = \frac{j\alpha}{\omega\epsilon}$$

Equation 4. 7

To support TM surface waves, surface impedance should be inductive (positive reactance), so materials with negative permittivity don't support TM surface wave. From duality principals for TE surface wave we can extract similar results. In TE wave we need to consider Magnetic field instead of Electric field and permeability instead of permittivity. Surface impedance for TE wave is gained using following expression:

$$Z_s = \frac{-E_y}{H_z}$$

Equation 4. 8

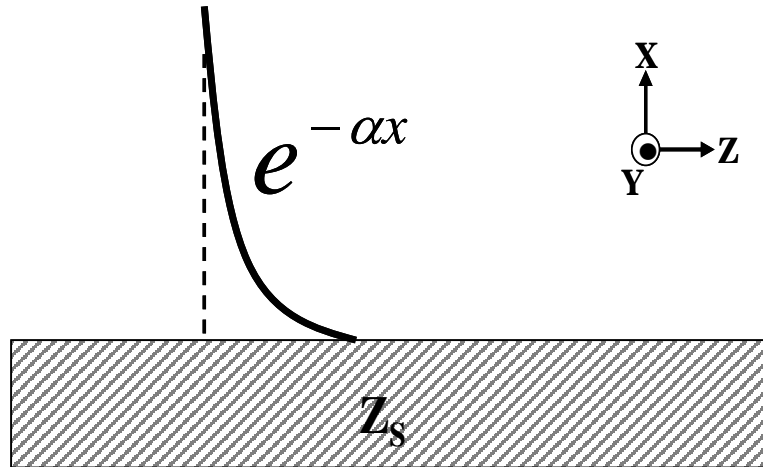


Figure 4. 10. Propagation of surface wave on an interference of two dissimilar materials



Therefore the surface impedance is:

$$Z_s(TE) = \frac{-j\omega\mu}{\alpha}$$

Equation 4. 9

To support TE surface waves, surface impedance should be capacitive (negative reactance), so materials with negative permeability don't support TE surface wave. EBG structures act as negative materials (medium with either negative  $\mu_r$  or negative  $\epsilon_r$ ) in the gap to suppress surface waves.

EBG structures around the gap show high impedance surface. Impedance for equivalent LC model of Figure 4. 3 is showed by:

$$Z = \frac{j\omega L}{1 - \omega^2 LC}$$

Equation 4. 10

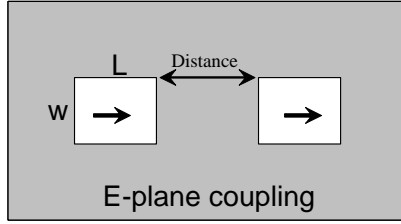
This impedance is inductive at low frequencies and it supports TM surface waves and it is capacitive at high frequencies and it supports TE surface waves. Around the resonance frequencies the surface impedance is high and it suppress the propagation of waves.

#### 4.4. EM wave mitigation using EBG materials

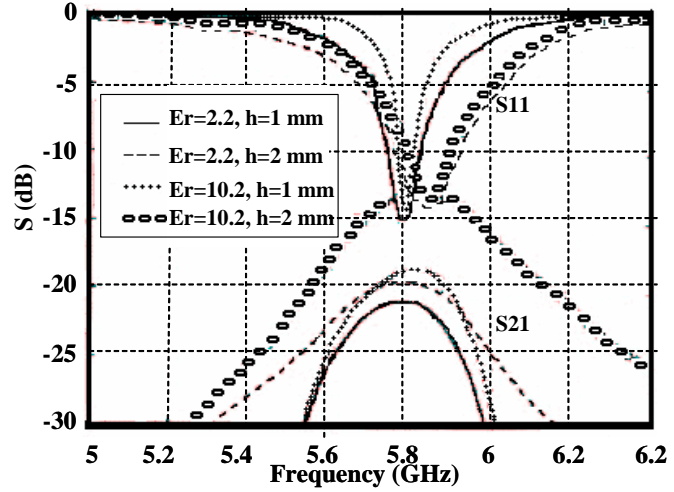
Following the efficiency of EBG structures for EM interference reduction is illustrated. This capability is showed through several applications proposed by other researchers.

##### 4.4.1. Antenna

Patch antenna on high dielectric constant substrate is preferable because of its compact size. Also thick substrate can improve the antenna bandwidth. However these specifications excites surface wave and causes intense mutual coupling between arrays of microstrip antennas. Analysis and experiments have showed EBG structure with appropriate gap and position is useful in suppression of coupling in E-plane and H-plane configuration in high permittivity and thick substrates. It is showed [6] in E-plane configuration the mutual coupling is increased when the permittivity or thickness of substrate is increased shown in Figure 4. 11. In H-plane configuration the mutual coupling becomes greater by increasing the substrate thickness but coupling decreases by increasing the substrate permittivity shown in Figure 4. 12. The EBG structure with the band gap on frequency which patch antenna is working effectively mitigates the surface wave and decreases coupling. As it is clear in Figure 4. 13 the gap produced by 2.5 mm and 3 mm patches are appropriate for this purpose.

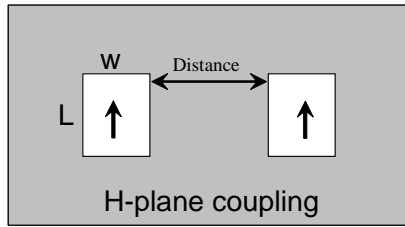


(a)

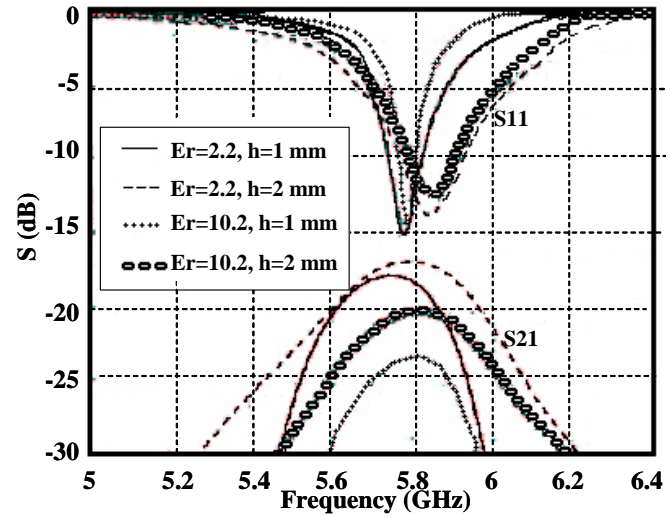


(b)

Figure 4. 11.(a) E-plane coupled probe fed patch antenna, (b) Comparisons of E-plane coupled patch antennas on different permittivity and thickness substrate, magnitude of S11 and S21 vs. frequency when the distance between antennas is  $0.5\lambda_0^1$



(a)



(b)

Figure 4. 12. (a) H-plane coupled probe fed patch antenna, (b) Comparisons of H-plane coupled patch antennas on different permittivity and thickness substrate, magnitude of S11 and S21 vs. frequency when the distance between antennas is  $0.5\lambda_0^2$

<sup>1, 2</sup> These figures have been taken from ref. [6]

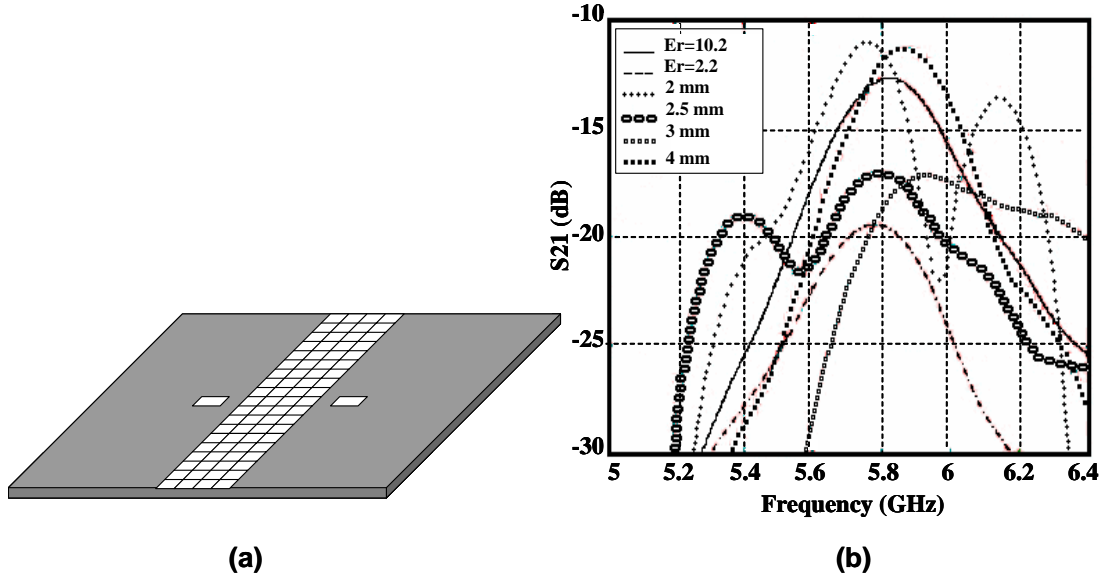


Figure 4. 13. Mutual coupling reduction by EBG structures with different patch sizes:  
(a) geometry, (b) Magnitude of  $S_{21}$  obtained by FDTD simulation<sup>1</sup>

Similar result has been obtained in other investigations have been done for reduction of coupling noise in other types of antennas. EBG can suppress surface wave producing significant edge diffraction in Global Positioning System (GPS) antennas [7]. Then there is a shield against the multipath noise. Also it is showed in [9] that EBG, which serves as a ground plane in the portable handset prototype, suppress surface waves. Figure 4. 14 shows handset antenna, which is a copper wire, etched on the FR4 board. This antenna is located on the EBG structures and it is integrated to the circuit board to minimize cost.

<sup>2</sup> This figure has been taken from ref. [6]

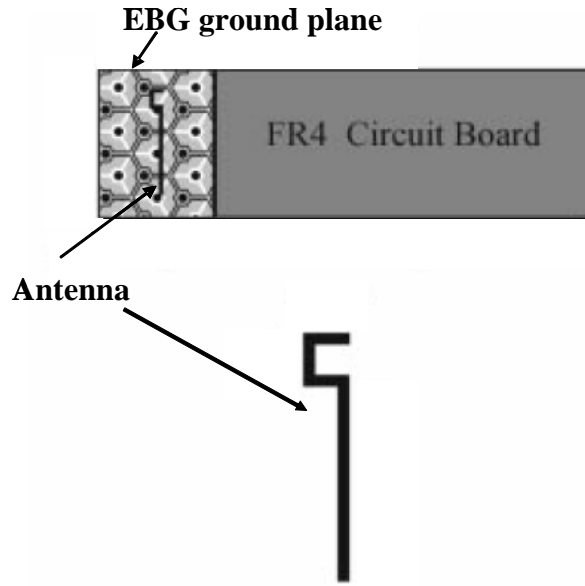


Figure 4. 14. Portable handset prototype with EBG ground plane<sup>1</sup>

Studies in [10] showed, these structures enable the coexistence of 802.11b and Bluetooth antennas on the laptops as well. The Bluetooth wireless antenna is used for short range of applications such as wireless print and cordless keyboard and mouse operations and hoc networking. The 802.11b wireless antenna is used to provide wireless internet access. Investigations in that study proved two antennas can be isolated by minimum 45 dB in the 2.4GHz ISM band (2.4-2.48 GHz) by implementing EBG materials on the laptop. In that experiment, 16 mm wide screen laptop housing was used and two 2.4 GHz antennas were mounted on the top and side of that screen as showed in Figure 4. 15. The dimensions of antennas and EBG cells used in this modeling are 37 x 12 x 3.4 mm and 55 x 12 x 2.5 mm respectively. The result of measurement is showed in Figure 4. 16.

<sup>1</sup> This figure has been taken from ref. [9]

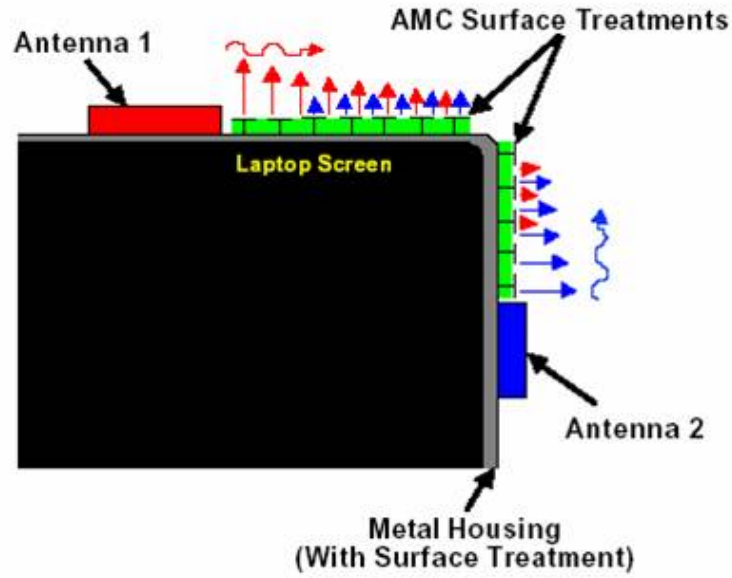


Figure 4. 15. Artificial Magnetic Conductor (AMC) surface treatments (EBG structures) impede surface waves<sup>1</sup>

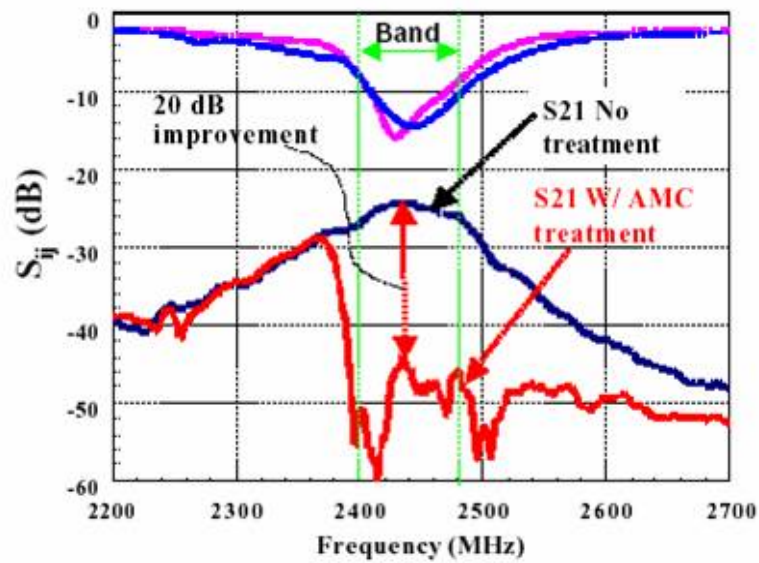


Figure 4. 16. Measured return loss and mutual coupling for the antennas shown in Figure 4. 15<sup>2</sup>

<sup>1, 2</sup> These figures have been taken from ref. [9][10]

#### 4.4.2. Power planes and Printed Circuit Boards

In high-speed digital systems compliance to EMC standards is one of the challenges. Increase in clock and bus speed is caused that circuit radiates by lower wavelength. Also power consumption is considerable in today's electronics therefore it is investigated to lower the voltage level in components. Typically several gates switch simultaneously in electronic circuits and they produce noise that affects on performance of the components connected to power plane. Also the vias passing through the layers of PCB without any connection to the power planes can be another source of noise. When the noise produced in parallel planes approaches tolerance limit of the CMOS components or the noise produced by active devices contains dominant modes of the parallel planes, signal integrity and performance of electronic circuits in the board will be degraded. Also layers of PCB radiates like a patch antenna. Techniques of applying EBG structure have proposed efficient solutions to mitigate noise in power planes and PCBs. To overcome noise in power planes one of the plates of parallel power plane pair is replaced with EBG structures [11], [12], [14], [15] shown in Figure 4. 17. These structures are needed to provide relevant band gap to suppress the resonant modes of the power planes. In PCBs the EBG structures like a ribbon are located around the board to suppress radiation from board (Figure 4. 18) [13]. These techniques efficiently reduce EMI in layers of board and propose an efficient solution for switching noise and radiation from PCBs which are major concerns for EM compatibility.

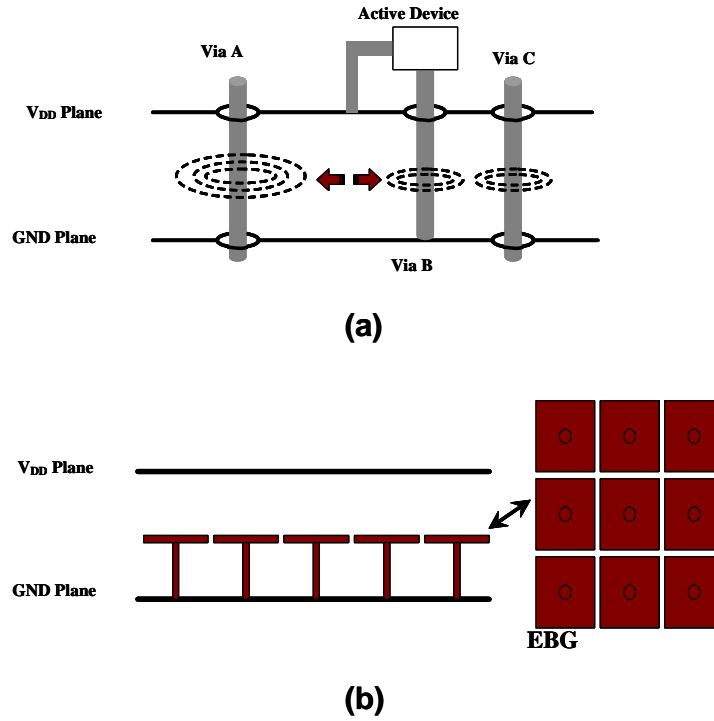


Figure 4. 17. (a) Traditional power planes with connecting vias, (b) Power planes with EBG plate. The EBG plane is used to suppress the switching noise and noise induced from active devices or vias that passes through power planes

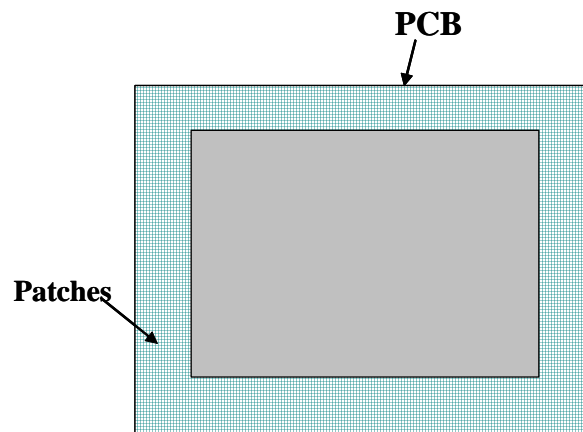


Figure 4. 18. Top view of printed circuit board with a ribbon of EBG around it, this ribbon is used to suppress the radiation from PCB to provide shielding



#### 4.4.3. Signal Integrity on PCBs

A perforated ground plane, which resembles EBG structures, is used to suppress the coupling between adjacent and intersecting microstrip transmission lines in PCBs [8]. These structures produce band gaps around the frequency ranges carried by each transmission line which mitigates coupling interference.

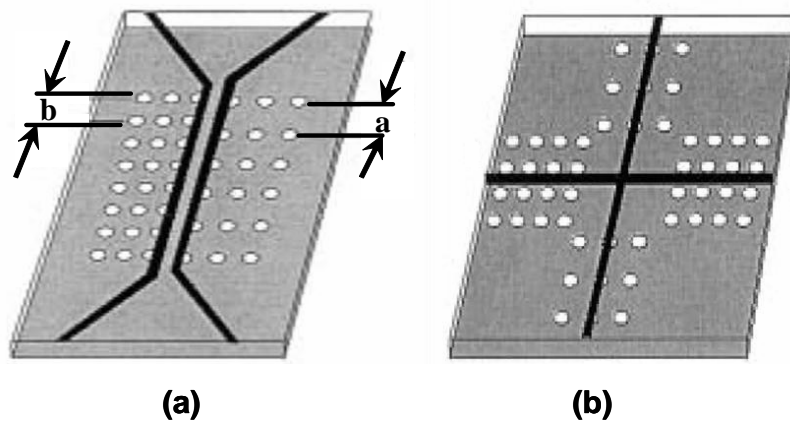


Figure 4. 19. (a) Two adjacent microstrip transmission lines on the perforated ground plane, (b) two intersecting microstrip lines on the perforated ground plane.

Perforation, which resembles EBG structure, suppresses coupling interference and cross talk between lines<sup>1</sup>

---

<sup>1</sup> This figure has been taken from ref. [8]

## Chapter 5 : Application of EBG Materials for EM Noise

### Suppression

#### 5.1.New EMI Shielding Approach in Enclosures Using EBG

As mentioned earlier implementing the lossy material and absorbers has provided excellent shielding effect in many applications, however, mechanical and heat irresistibility of these materials providing limited lifetime. EBG structures far from these problems have provided solution to the shielding scenarios. If the route of coupling interference is recognized EBG structures can be implemented to impede flow of surface current providing gap in relevant operating frequencies.

##### 5.1.1. Methodology

The concept of implementing EBG patterns on the package to shield the system by blocking the flow of current on the enclosure surface, which is the source of resonance and radiation in the enclosures and apertures, is the novel method for shielding purpose. Mechanism of coupling between the interior electromagnetic source and the external electromagnetic environment is through direct penetration of field through openings or through induced current on package surface. This current can excite resonance modes of the cavity enclosure or apertures and it can be radiated from edges, discontinuities and non-uniformities to the environment. We approach this concept by implementing EBG pattern on the package and chassis, which shields

the system by blocking the flow of current as the source of resonance and radiation on the enclosure surface. The proposed technique is to cover the enclosure all around by a ribbon of EBG structures. This ribbon is isolating openings and apertures similar to an island and provides a forbidden gap for current flow between interior and exterior of the package.

Figure 5. 1 shows the enclosure box covered with two EBG ribbons. To investigate the idea, we carry on an experiment. To setup a test with surface current as a major source of interference one enclosure, which attached back to back to similar one, is excited by a probe and the coupled field is captured in other enclosure. S12 in this configuration shows the interference coupling. Figure 5. 2.(a) shows method of connecting two boxes to each other and Figure 5. 2.(b) shows the experiment setup when the boxes covered with a ribbon of EBG all around.

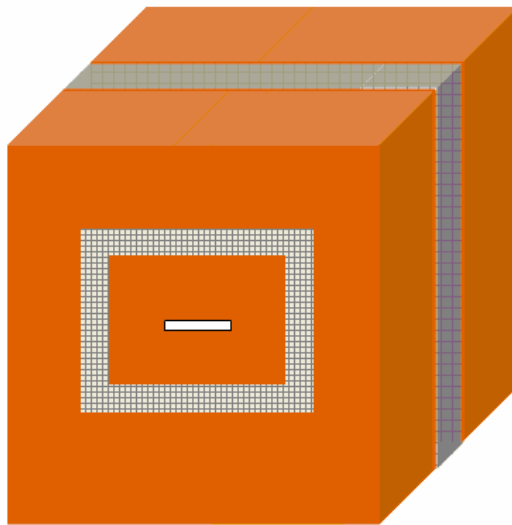


Figure 5. 1. Test Enclosure; box with Two EBG ribbons

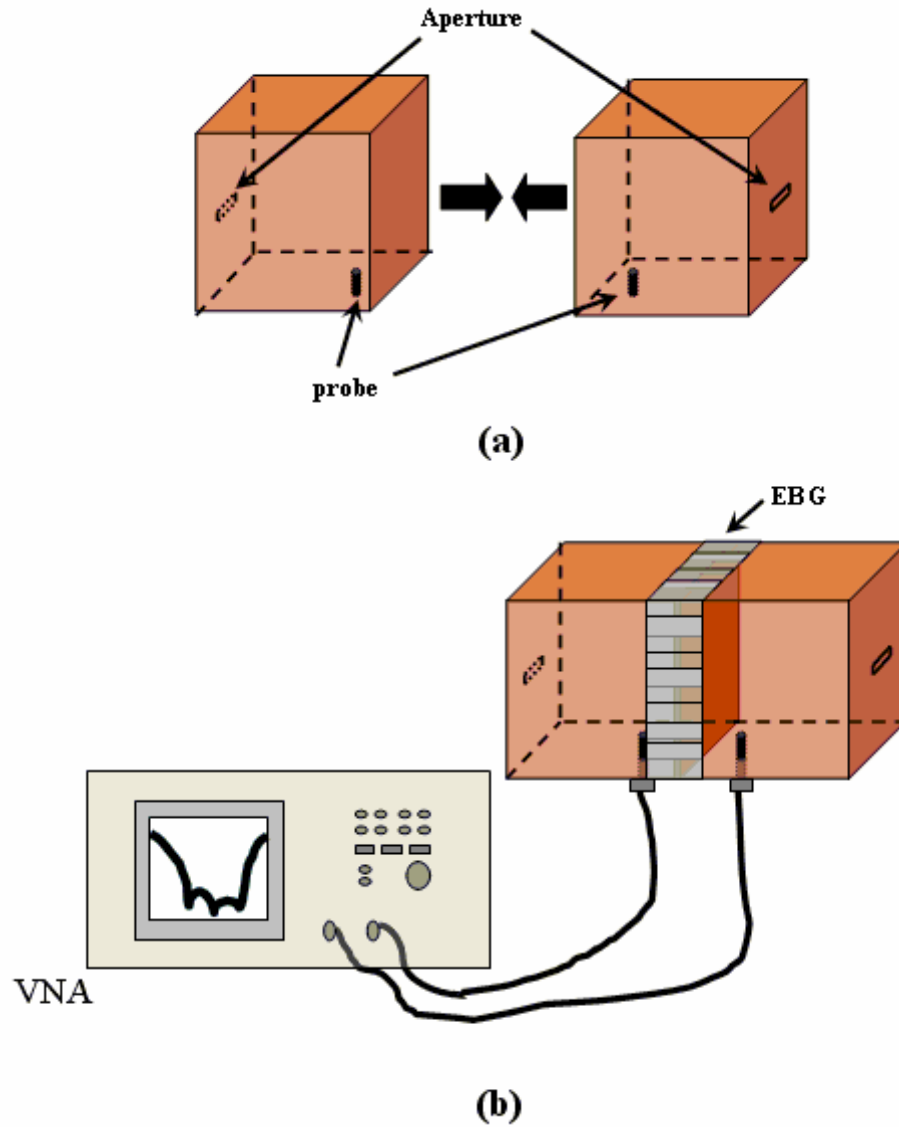


Figure 5. 2. (a) Schematic of connecting two cavity boxes to each other for an experiment, (b) Boxes covered with an EBG ribbon all around to investigate efficacy of EBG material for the interference coupling suppression

### 5.1.2. Numerical Simulation and Validation

Here we follow the proposed experiment numerically. The size of each box is 8 x 16 x 6 cm, the size of aperture is 30 x 4 mm and the probe is located at the side of box at the distance of 2 x 2 cm from edge. The configuration of two boxes is symmetric.

Table 5. I. The specification of unit cell of the EBG pattern

| Pattern | $\epsilon_r$ | t (mm) | a (mm) | g (mm) | Via type & d (mm) | Stop band GHz |
|---------|--------------|--------|--------|--------|-------------------|---------------|
| 1       | 2.2          | 1.54   | 4      | .4     | Cubic & .8        | 8.4-9.6       |
| 2       | 4.8          | 1.54   | 4      | .4     | Cubic & .8        | 6.5-7.5       |

The specification of EBG patterns (for more information refer to Figure 4. 1): a, d, g, t, via type and dielectric permittivity which provide desired stop bands for our purpose is given in Table 5. I. Without loss of generalization, and in order to reduce the computational burden in the full-wave simulations, we have considered cubic instead of cylindrical vias. Figure 5. 3 and Figure 5. 4 show the dispersion diagrams of EBG pattern #1 and #2 respectively. Dispersion diagram that shows relation between wave number and frequency illustrates modes and band gaps if possibly exists between modes. In the dispersion diagrams the free space frequency-wave number line shows the free space speed limit. Therefore the gap between upper limit of TM mode and intersection of this line with TE mode shows forbidden region, irrespective of the direction of propagation and polarization. The Attenuation bands,

which gained with this method, spread almost from 8.4 to 9.6 GHz and from 6.5 to 7.5GHz for specified patterns respectively.

A ribbon of mentioned EBG patterns is used around the box to show the suppression in the relevant band gaps. The width of ribbon is 44mm. The result of simulation is a confirmation of efficacy of the method for coupling mitigation. Figure 5. 5 and Figure 5. 6 show the results of simulation for traditional enclosure (blank case) besides the case those EBG patterns are implemented to the package. From results it can be seen in that application that surface current propagates in any direction the effective interference reduction band extends from 7.6GHz to 9.1 GHz in pattern # 1 and from 6.2GHz to 7.9 GHz in pattern # 2. The band of effective EMI reduction is comparable to band gaps extracted from the dispersion diagram. The difference is because of computational errors and phenomenon that it is not studied yet like negative slope in the dispersion diagram or negative group velocity. The maximum coupling suppression in gap is 35 dB for EBG pattern #1 and 23 dB for EBG pattern #2. The maximum coupling is defined as maximum over the entire band gap. This noticeable interference reduction certifies applicability of this method for shielding purpose.

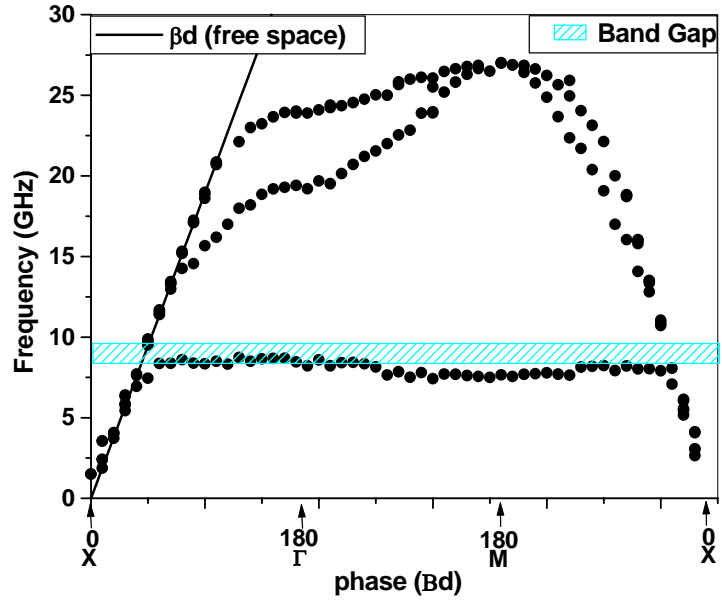


Figure 5. 3. Dispersion Diagram of EBG pattern with  $\epsilon_r = 2.2$ ,  $t = 1.54$  mm,  $a = 4$  mm,  $g = 0.4$  mm and cubic via with  $d = 0.8$  mm (Pattern #1)

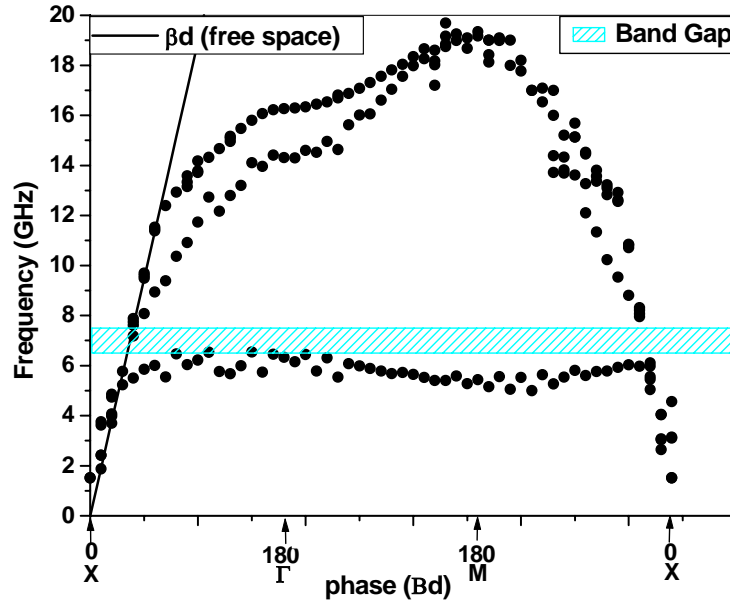


Figure 5. 4. Dispersion Diagram of EBG pattern with  $\epsilon_r = 4.8$ ,  $t = 1.54$  mm,  $a = 4$  mm,  $g = 0.4$  mm and cubic via with  $d = 0.8$  mm (Pattern # 2)

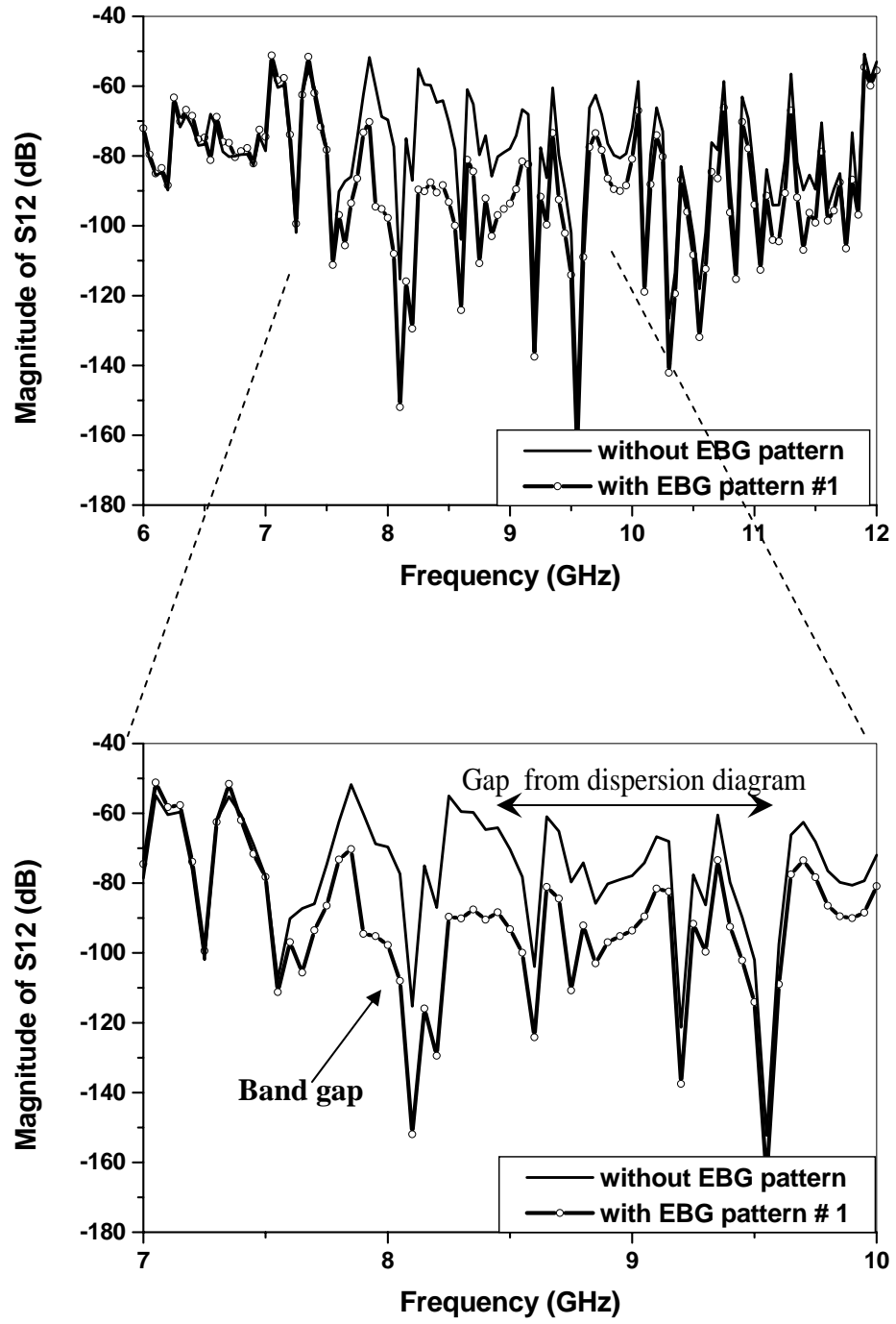


Figure 5. 5. shows the interference coupled inside the box from external source for two cases of with and without EBG patterns. Specification of EBG pattern #1 can be found in Table 5. I.



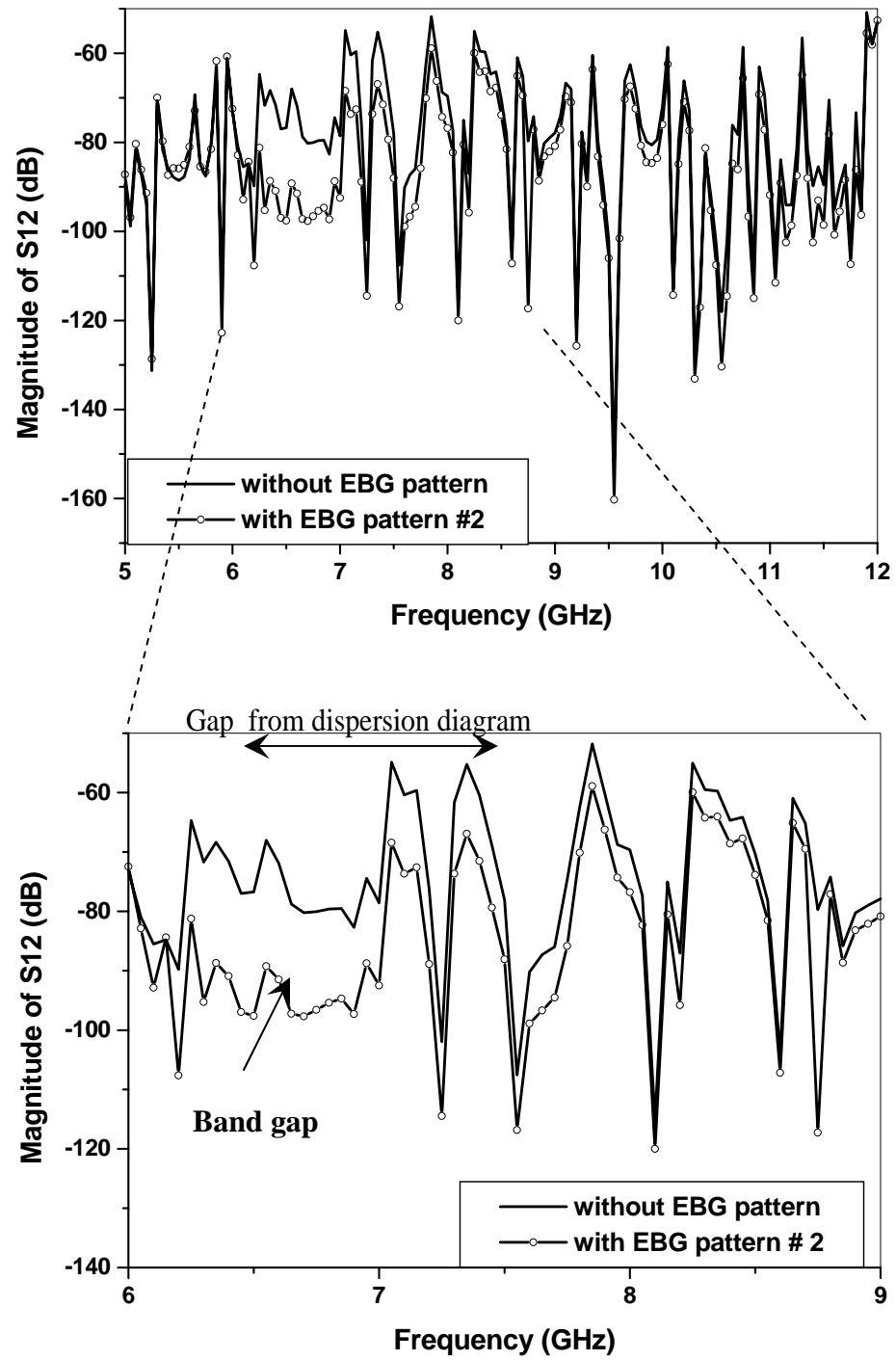


Figure 5. 6. shows the interference coupled inside the box from external source for two cases of with/out EBG patterns. Specification of EBG pattern #2 can be found in Table 5. I

## 5.2. Surface Wave Suppression in Cavity Backed Slot Antennas

Investigation on mitigation of surface waves on cavities is important for two purposes. First, two or more cavities next to each other resemble different compartments and partitions in the chassis. Second, cavity backed slot antenna is one type of antenna with the broad range of applications. Therefore we continue our studying by investigation on mutual coupling in cavity backed slot antennas.

Today we need complicated systems with several antennas or array of antennas and other electromagnetic sources in the same environment. However, installing a new EM source because of possibility of mutual coupling interference between them is a challenging task. As mentioned earlier in chapter 3 investigations in [1] showed that implementing lossy materials is much more effective than other classical methods for interference suppression. However we have heat and mechanical irresistibility of these materials. Here we investigate about interference coupling reduction technique by applying EBG materials to CBS antennas.

### 5.2.1. Methodology

To evaluate efficiency of the method of implementing EBG material for interference noise suppression the same geometry for CBS antennas as [1] is used. This geometry, which is showed in Figure 3. 3 for convenience is repeated in Figure 5. 7. As it is clear from S11 graph of Figure 5. 9.(a), this specified CBS antenna can work at 7.5GHz and 12.6 GHz. In simulation two CBS antennas mounted on the

finite ground plane of dimension 10x6 cm. Figure 5. 8 shows the geometry of two identical CBS antennas on a ground plane.  $S_{12}$ , which shows coupling between two antennas, is illustrated in Figure 5. 9.(b) . The space between two antennas is covered by EBG structures having band gap around the frequency which antenna is working. The geometry under examination is illustrated in Figure 5. 8.

As following result will show EBG patterns significantly reduces mutual interference by mitigating surface wave. However, here it is emphasized that gain pattern and directivity of antennas after implementing EBG structures are changing therefore it is important to consider the specification of antennas to satisfy efficiency of a communication system.

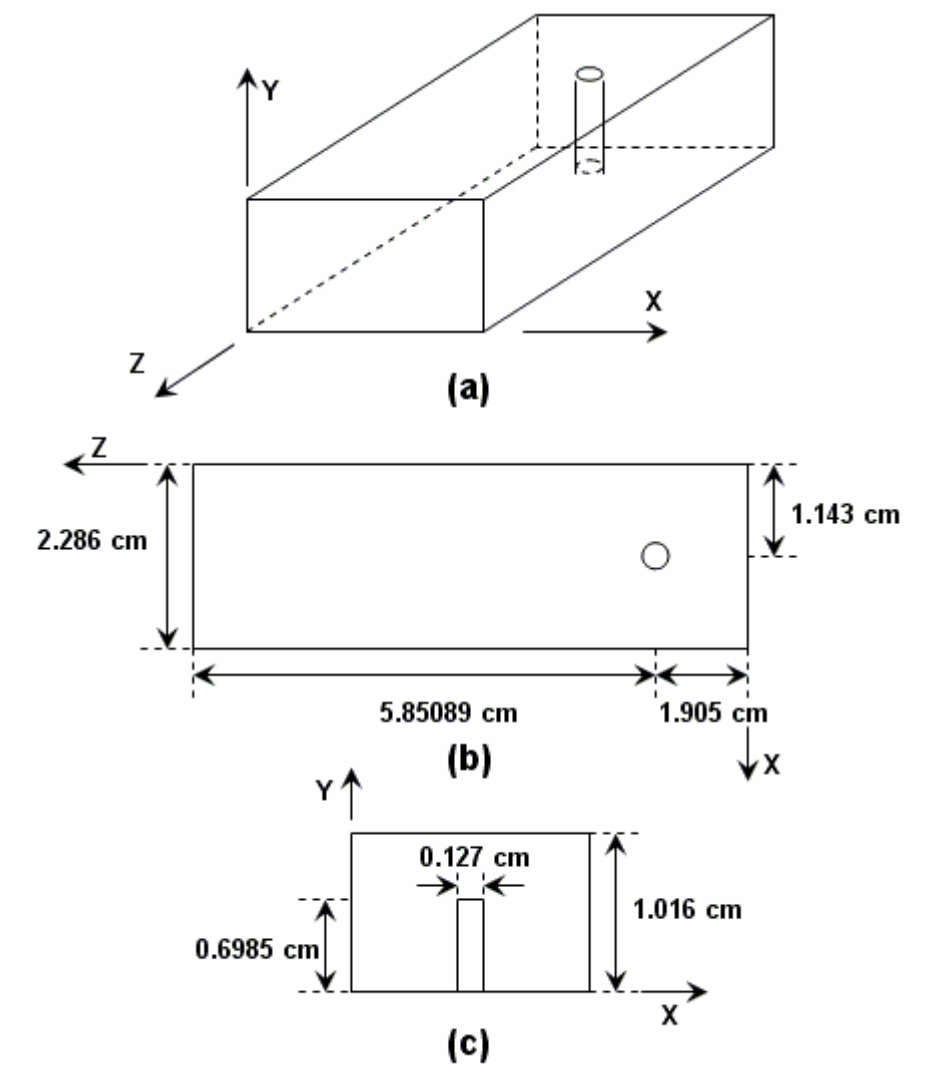


Figure 5. 7. Air-filled rectangular CBS antenna fed with probe oriented in the y-direction. (a) Perspective view, (b) top view and (c) side view of (xy-plane)

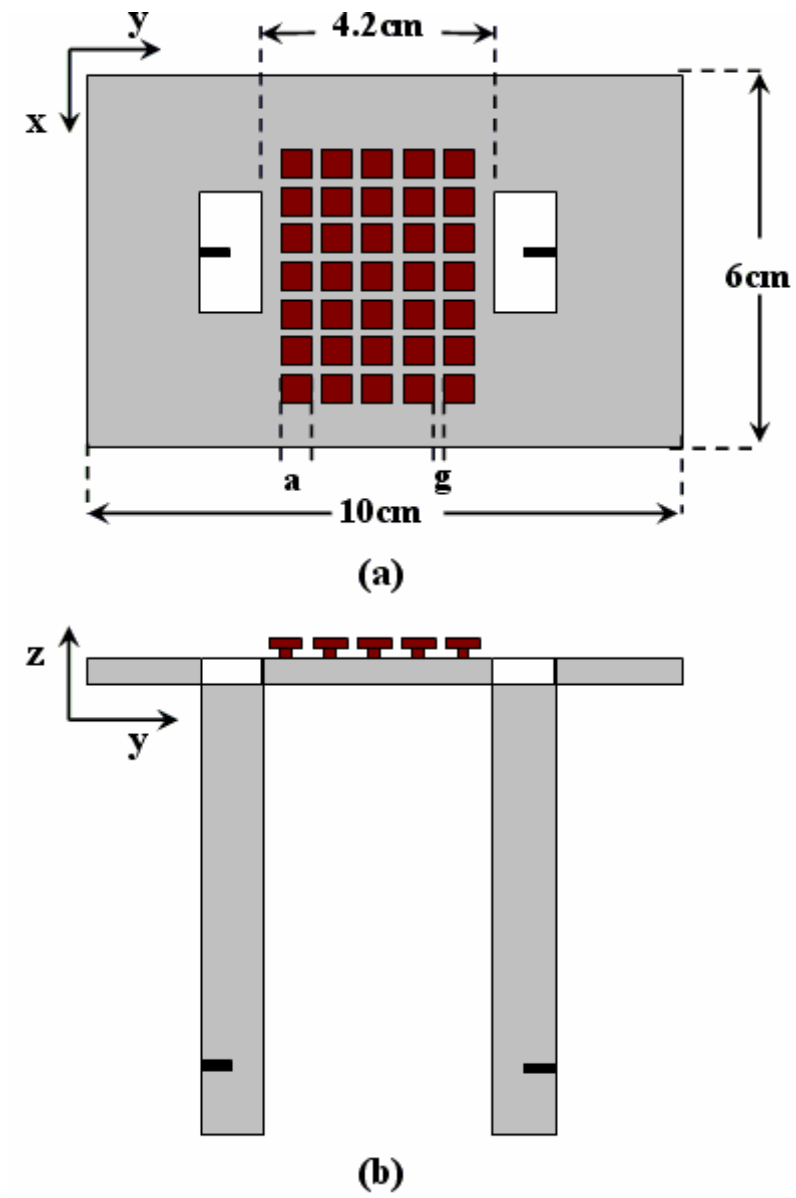
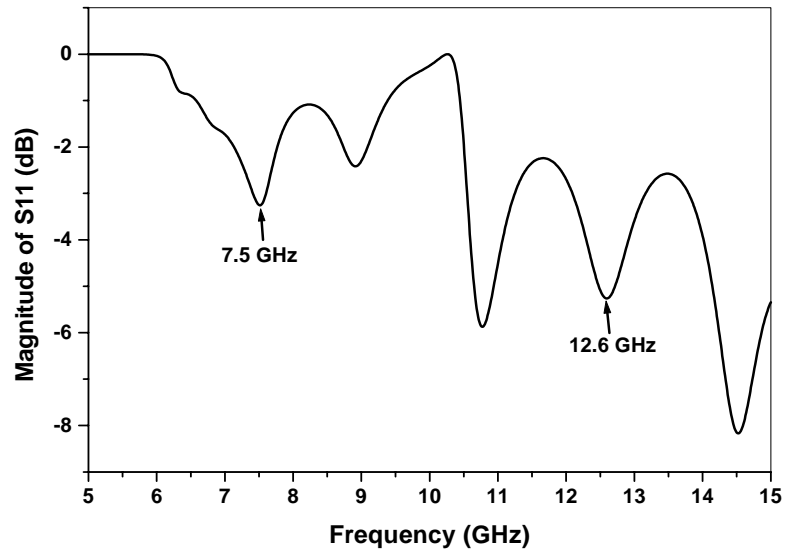
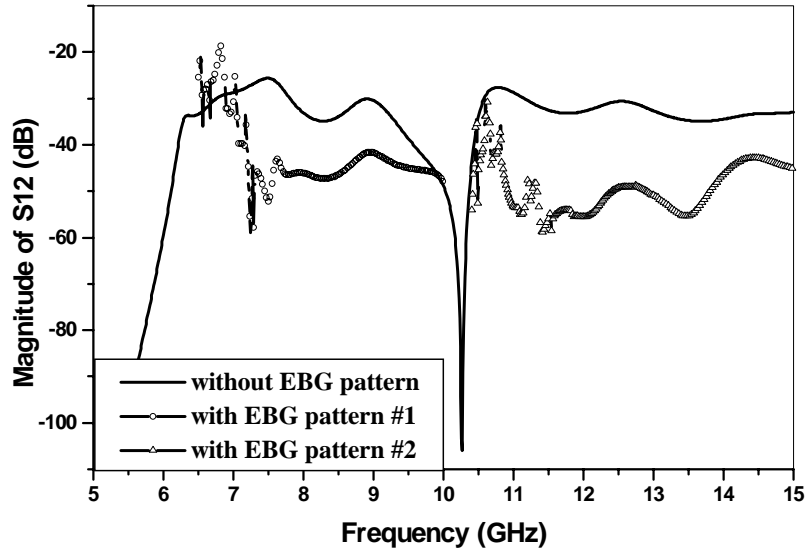


Figure 5. 8. Geometry of two identical CBS antennas mounted on EBG ground plane  
(for antenna specification see Figure 5. 7), (a) top view (b) perspective view



(a)



(b)

Figure 5. 9. (a) and (b) show S-parameters of two identical CBS antennas mounted on a rectangular ground plane (blank case), for antenna specification see Figure 5. 7. Antennas can operate at 7.5 and 12.6 GHz as marked on plot. Also (b) shows coupling between antennas when EBG ground plane is used. Two different EBG designs for these two operating frequencies are implemented to show efficiency of these materials in coupling reduction, (for EBG structures specification see Table 5. II). S-parameters extracted by HFSS simulation.

### 5.2.2. Numerical Simulation and Validation

It is clear from  $S_{11}$  in Figure 5. 9.(a) that the specified CBS antenna can work at 7.5GHz and 12.6 GHz. Similar to [1] coupling without implementing EBG material labeled “blank” for reference purposes (Figure 5. 9.(b)). In continue EBG pattern # 1 and # 2 that have gap around those optimum operating frequencies placed on top of the ground plane filling entire space between two slots. The specification of the EBG patterns (for more information refer to Figure 4. 1): a, d, g, t, via type and dielectric permittivity which provide desired stop bands for our purpose is given in Table 5. II. Figure 5. 10 and Figure 5. 11 show the dispersion diagrams of EBG pattern # 1 and # 2 respectively. In the dispersion diagrams the free space frequency-wave number line shows the free space speed limit. Therefore the gap between upper limit of TM mode and intersection of this line with TE mode shows forbidden region, irrespective of the direction of propagation and polarization. Therefore stop band spread almost from 7 to 8 GHz and from 11.9 to 17.3 GHz for pattern # 1 and # 2 respectively.

Table 5. II. The specification of unit cell of the EBG pattern

| pattern | $\epsilon_r$ | t (mm) | a (mm) | g (mm) | Via type &<br>d (mm) | Stop band<br>GHz |
|---------|--------------|--------|--------|--------|----------------------|------------------|
| 1       | 4.8          | 1.54   | 4      | .4     | Cylindrical<br>& .8  | 7-8              |
| 2       | 3            | 1.54   | 2.6    | .4     | Cylindrical<br>& .8  | 11.9-17.3        |

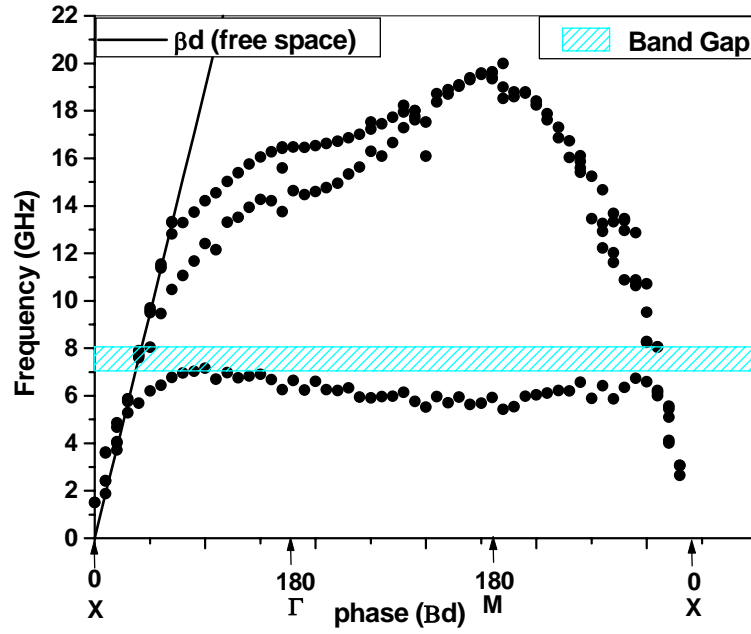


Figure 5. 10. Dispersion Diagram of EBG pattern with  $\epsilon_r = 4.8$ ,  $t = 1.54$  mm,  $a = 4$  mm,  $g = 0.4$  mm and cylindrical via with  $d = 0.8$  mm (Pattern #1)

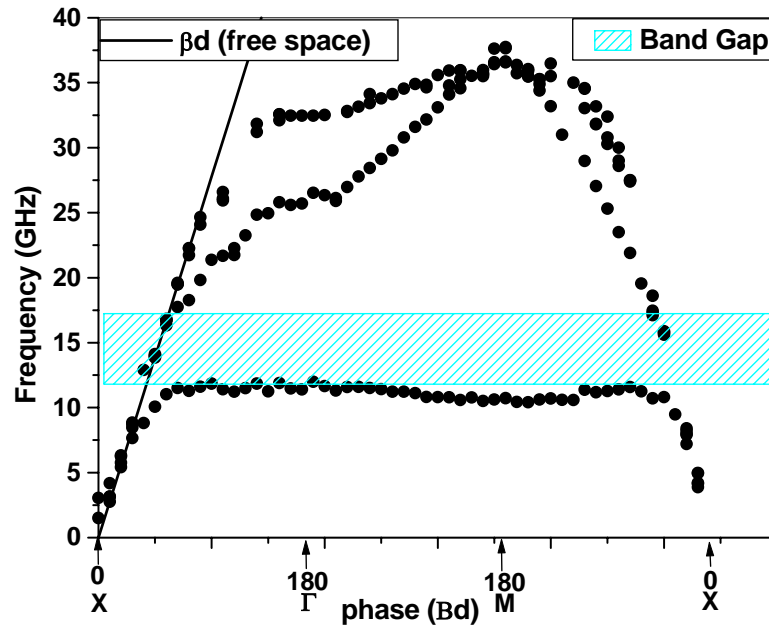


Figure 5. 11. Dispersion Diagram of EBG pattern with  $\epsilon_r = 3$ ,  $t = 1.54$  mm,  $a = 2.6$  mm,  $g = 0.4$  mm and cylindrical via with  $d = 0.8$  mm (Pattern #2)



The result of simulation is illustrated in the Figure 5. 9.(b). The coupling reduction of 25 dB for EBG pattern # 1 and 20 dB for EBG pattern # 2 are obtained in band gaps at operational frequencies of antennas. Also, the maximum coupling reduction of 33 dB for EBG pattern # 1 and 27 dB for EBG pattern # 2 are gained in suppression bands of these materials, which are quite noticeable. It is enough to mention that refer to section 3.2.1 the largest coupling reduction of 7dB obtained by applying lossy material to antennas. However, since then ever going researches in material science has introduced better materials to market. Figure 5. 12 and Figure 5. 13 show surface current density  $J_{tot}$  on the ground for the two case of with/out EBG at 7.5 GHz and 12.6 GHz respectively. Surface current, which couples energy from one CBS antenna to another, is banded perfectly in the gap provided by EBG structures. At 7.5 GHz in blank case  $J_{tot}$  of about 0.8 A/m (-2dB) establishes a strong coupling however, maximum current reduces to 0.3 A/m (-10dB) by using EBG, which confirms coupling reduction mechanism. At 12.6 GHz  $J_{tot}$  reduces approximately from 0.5 A/m (-6dB) to 0.15 A/m (-16dB).

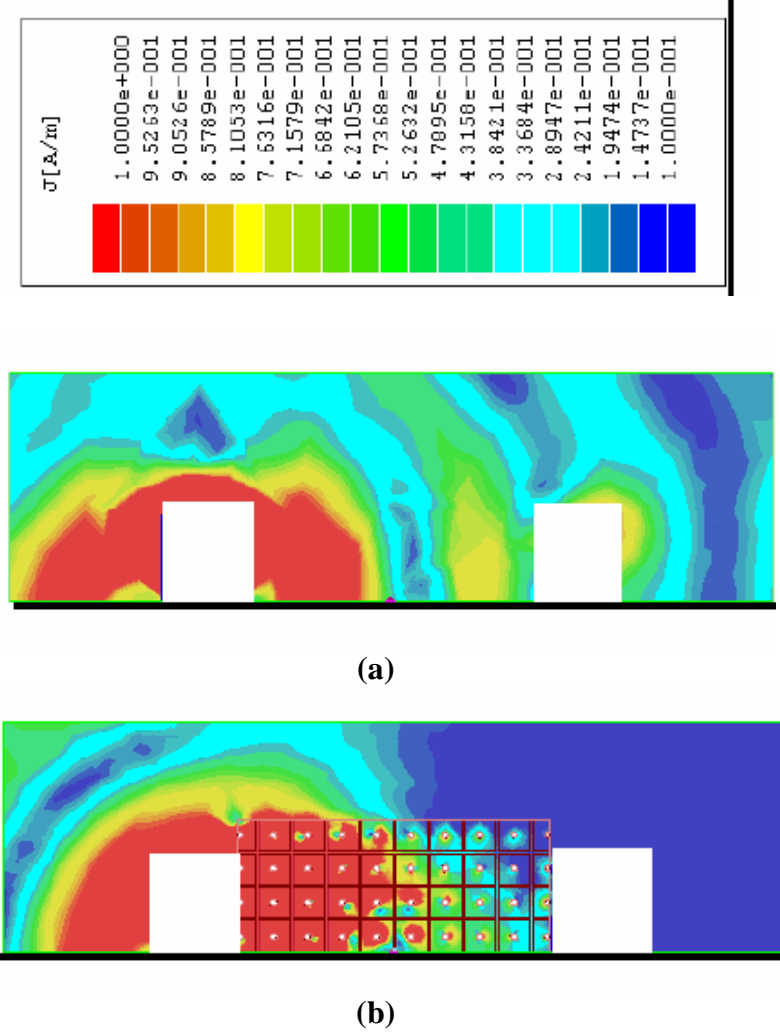


Figure 5. 12. Total surface current density ( $J_{tot}$ ) (a) on the blank ground plane and (b) on the EBG ground plane when the CBS antenna is working at 7.5 GHz. The EBG pattern # 1 provides efficient gap at this frequency. For EBG structure specification see Table 5. II

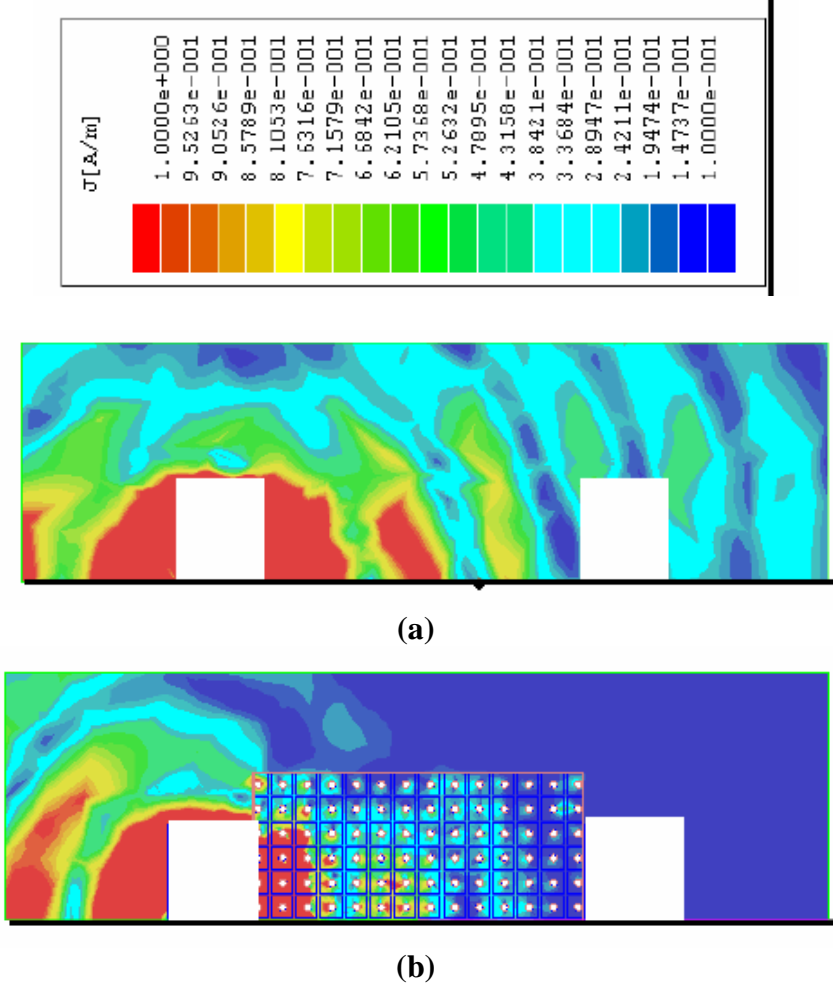


Figure 5. 13. Total surface current density  $J_{tot}$  (a) on the blank ground plane and (b) on the EBG ground plane when the CBS antenna is working at 12.6 GHz. The EBG pattern # 2 provides efficient gap at this frequency. For EBG structure specification see Table 5. II

Use of EBG patterns in the space between two CBS antennas varies the geometry therefore radiation pattern in antennas. This variation is relevant to degree of vicinity of EBG structures to the antennas to block the radiation angle. In our studies, which two antennas are close to each other while whole space between them filled with EBG materials, these changes are more noticeable. It is expected the antenna with EBG ground plane radiates more directional and with better gain in some observation angles. However, gain reduction is predicted toward the EBG patterns because of prohibition in flow of energy. Radiation pattern of CBS antenna computed for two cases of with/out EBG material. These patterns are illustrated in Figure 5. 14 and Figure 5. 15 at 7.5 GHz and 12.6 GHz respectively. To get pattern only one of the antennas was excited. Simulation results confirm our prediction.

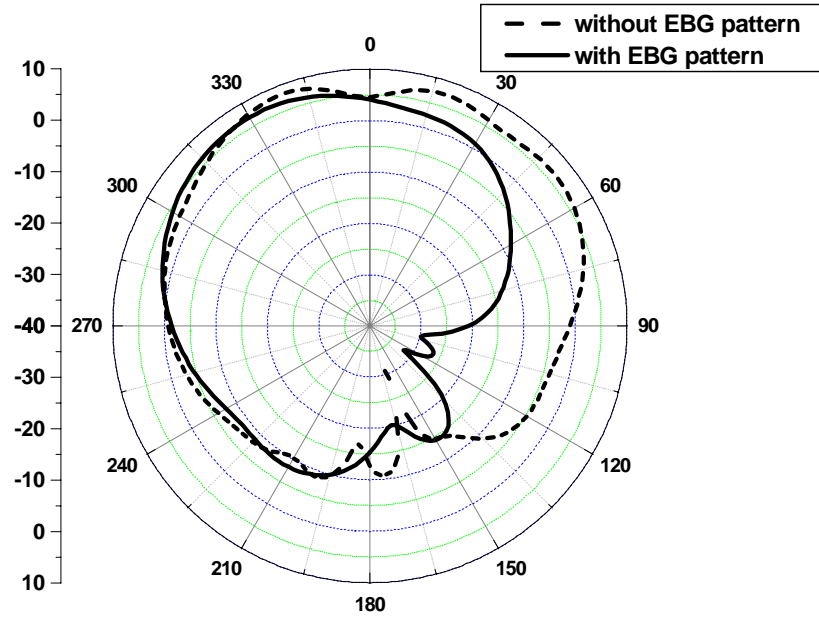


Figure 5. 14. The antenna gain patterns at 7.5 GHz with/out EBG structures. The EBG pattern # 1 provides efficient gap at this frequency. For EBG structure specification see Table 5. II

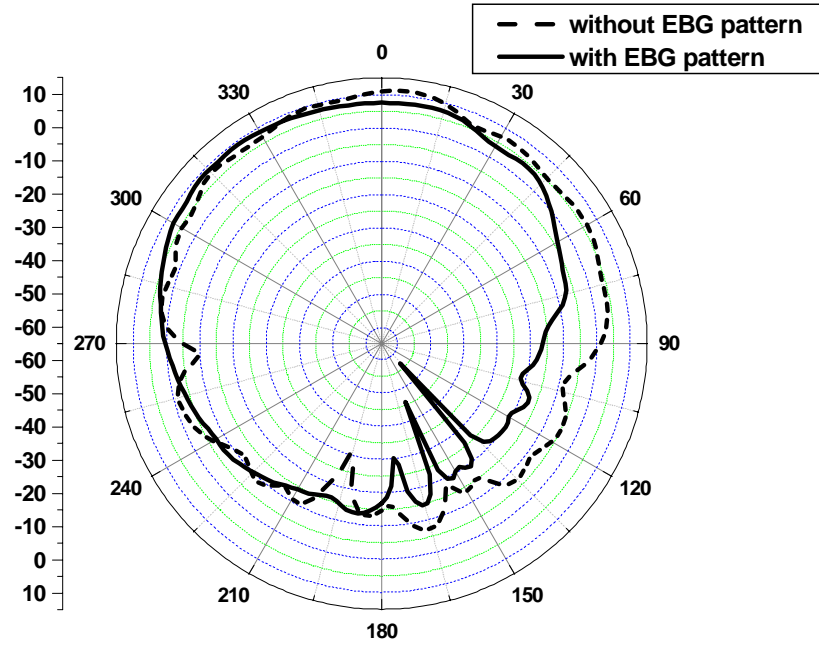


Figure 5. 15. The antenna gain patterns at 12.6 GHz with/out EBG structures. The EBG pattern # 2 provides efficient gap at this frequency. For EBG structure specification see Table 5. II

Looking at the gain in different observation angles clarifies that maximum increment of 2 dB and decrement of 18 dB at 7.5 GHz, and maximum increment of 4 dB and decrement of 18 dB at 12.6 GHz are obtained. Figure 5. 14 shows for the antenna working at 7.5 GHz, for observation angles  $-90 < \theta < 50$ , both increment and decrement in gain is around 4 dB and Figure 5. 15 shows for the antenna working at 12.6 GHz, for observation angles  $-90 < \theta < 30$ , decrement in gain is around 5dB and increment in gain is around 2 dB which is comparable with gain reduction of 5 dB reported by using lossy GDS in [1]. Observation angles  $50 < \theta < 90$  at 7.5 GHz and  $30 < \theta < 90$  at 12.6 GHz are almost blocked by EBG structures implemented to

antennas. Consequently there is a trade off between gain and coupling reduction in some angles in propagation space. However design of directive antennas become possible by using capability of EBG materials in blocking of surface wave.

Figure 5. 16 and Figure 5. 17 show propagation of wave in the free space and the ground plane at 7.5 GHz and 12.6 GHz respectively. In above figures, part (a) shows blank case and part (b) shows EBG ground plane case. As it is clear from radiation gain patterns, CBS antenna emits to all directions in upper half free space and EBG patterned plane directs the wave to other sides. Figure 5. 14 and Figure 5. 15 confirm this conclusion and provide good view about blocking of wave propagation using EBG pattern on the observation angles directing to these structures. Therefore coupling interference noise is eliminated considerably in this system.

Validation of applicability of EBG in interference suppression in CBS antennas mounted on the same ground plane shows EBG patterns can be used for EMC purpose in different electrically separated parts and housing inside the enclosures.

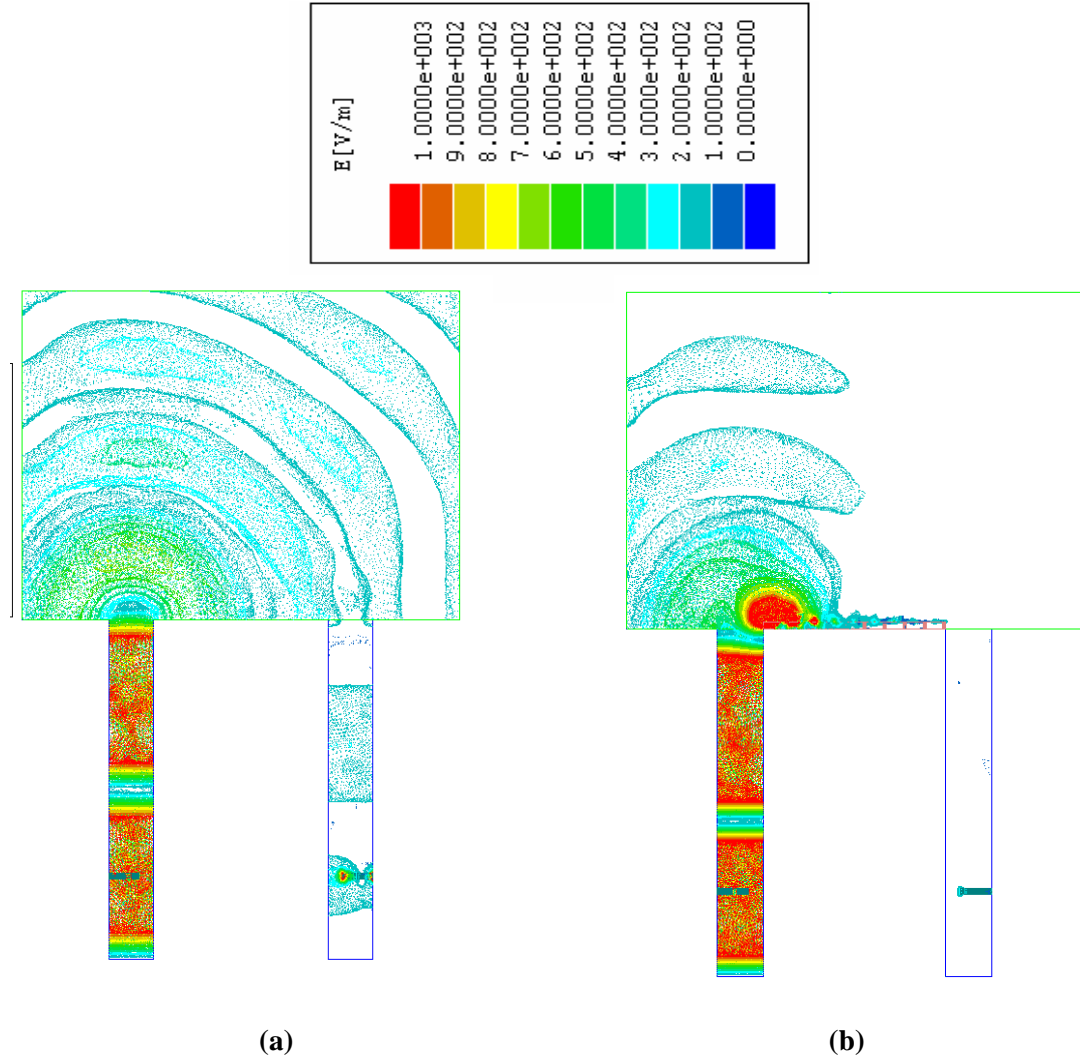


Figure 5. 16. Propagation of wave in the free space and on the ground plane when CBS antenna is working at 7.5 GHz in two case of (a) blank and (b) EBG ground plane. The EBG pattern # 1 provides efficient gap at this frequency. For EBG structure specification see Table 5. II

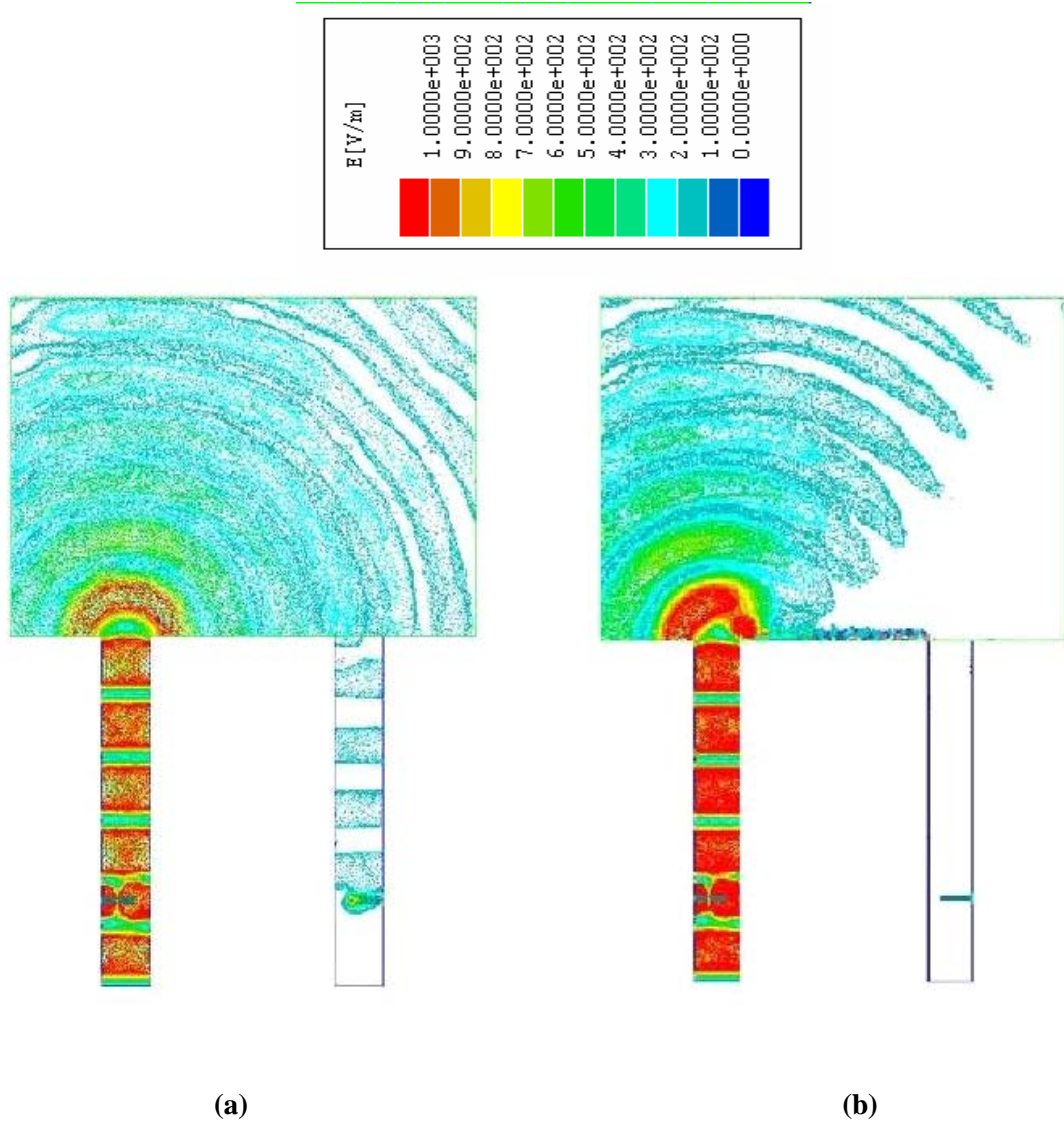


Figure 5. 17. Propagation of wave in the free space and on the ground plane when CBS antenna is working at 12.6 GHz in two case of (a) blank and (b) EBG ground plane. The EBG pattern # 2 provides efficient gap at this frequency. For EBG structure specification see Table 5. II



### 5.3. Effect of two different Configurations of the same EBG Pattern on the Band Gap

#### 5.3.1. Configurations

Two different topologies of the same EBG pattern are considered for coupling reduction in CBS antennas. If the propagating surface wave at the border encounters the vias, the major inductive part of the EBG pattern, this configuration (Figure 5. 18.(a)) is named Inductive ground plane. If the surface wave encounters patches at the border (Figure 5. 18.(b)), that one named Capacitive ground plane. Interestingly efficiency of Inductive and Capacitive EBG ground planes in suppressing coupling interference are different. This conclusion provides a new sight for applying EBG patterns for EMI purpose.

#### 5.3.2. Simulation Result

The simulation for a CBS antenna working at 7.5 GHz showed that Inductive EBG is more effective than Capacitive EBG in suppressing coupling noise. Comparison of the results of two configurations in Figure 5. 19 illustrates maximum difference of 25 dB in coupling reduction could be gained in the entire suppression band and if two antennas are working at 7.5 GHz difference of 10 dB in coupling interference is shown in this simulation. These differences are noticeable in interference blockage.

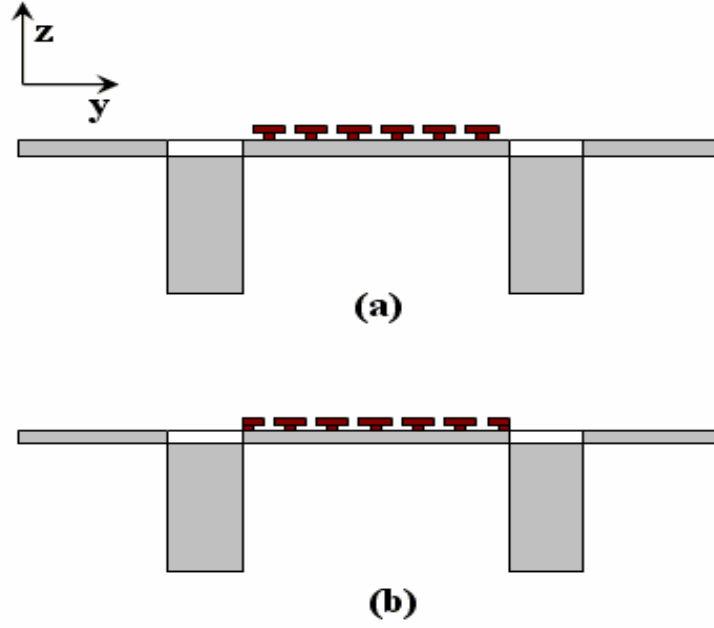


Figure 5. 18. Two identical CBS antennas mounted on (a) Capacitive EBG ground plane, (b) Inductive EBG ground plane

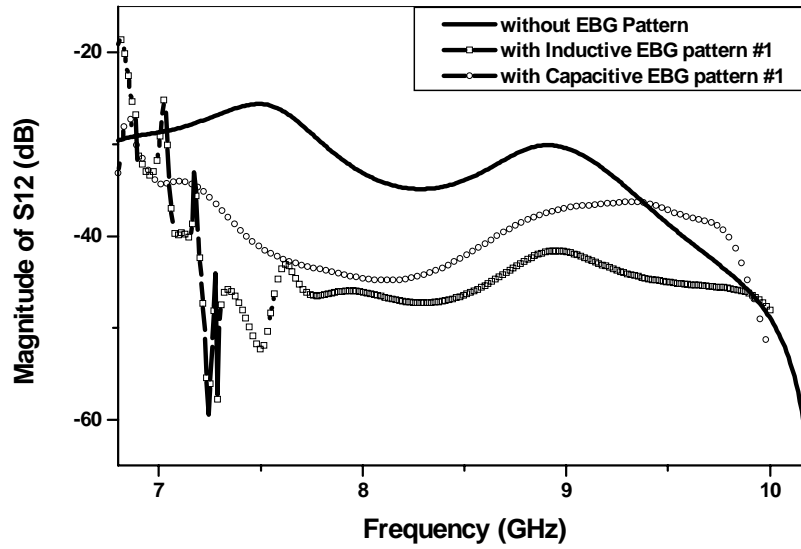


Figure 5. 19. Coupling Interference noise between two CBS antennas for three cases: I. Blank ground plane, II. Inductive EBG ground plane and III. Capacitive EBG ground plane. The CBS antenna is working at 7.5 GHz. The EBG pattern # 1 provides efficient gap at this frequency. For EBG structure specification see Table 5. II. For antenna specification see Figure 5. 7

## Chapter 6 : Summary and Future work

This study has presented a novel concept of using EBG structures for interference coupling mitigation in enclosures and cavities. This methodology provides reliability in high speed, low threshold voltage level electronic devices. The surface current which is created by radiated EM wave on metallic surfaces or supported by surface or traveling wave is blocked on the band gap provided by these structures. The results validate efficacy of this method providing shielding in enclosures and packages. Also we looked at mutual interference noise reduction in cavity backed slot antennas which is a perfect model for several set of problems (e.g., different compartment and partitions in a chassis or array of antennas). In addition to interference suppression we considered directivity and gain patterns of the cavity backed slot antennas. Applying EBG structures direct propagation and improve radiation on some observation angles which it makes the design of directive antennas possible. These changes depend to vicinity of EBG patterns to cavity slots. Also it is showed Inductive ground plane is much more effective than Capacitive one in EMI reduction. Therefore by changing topology of the same structure we can provide better efficiency in EMC applications.

As a comment it should be emphasized all the numerical results are gained with simplest form of EBG structures. Using EBG structures with optimized dimensions, patterns and materials can provide much more effective bands of suppression. So the results provided in this work are only for showing the ideas.

Doing measurements to confirm the results gained through the simulations presented in this work is the next step in our research. Validation of efficiency of this method in practice can direct our studies to new ideas.

## Bibliography

- [1] S.V. Georgakopoulos, C.R. Birtcher and C.A. Balanis, "Coupling modeling and reduction techniques of cavity-backed slot antennas: FDTD versus measurements," *IEEE Trans. Electromagn. Compatibility*, vol. 43, no. 3, pp. 261-272, Aug. 2001.
- [2] J.F. Dawson, J. Ahmadi and A.C. Marvin, "Reduction of radiated emissions from apertures in resonant enclosures by the use absorptive materials," *IEEE International Conference on Electromagnetic Compatibility*, pp. 207-212, Sept. 1992.
- [3] V. Adsure, H. Kroger and Shi Weimin, "Improving signal integrity in circuit boards by incorporating embedded edge terminations," *IEEE Transactions on Advanced Packaging [see also Components, Packaging and Manufacturing Technology, Part B: Advanced Packaging, IEEE Transactions on]*, vol. 25 , no. 1, pp. 12-17 , Feb. 2002.
- [4] Min Li, J. Nuebel, J.L. Drewniak, T.H. Hubing, R.E. DuBroff and T.P. Van Doren, "EMI reduction from airflow aperture arrays using dual-perforated screens and loss," *IEEE Transactions on Electromagnetic Compatibility*, vol. 42 , no. 2, pp. 135-141, May 2000.
- [5] D.F. Sievenpiper, High-impedance electromagnetic surface, Ph.D. Thesis, Department of Electrical Engineering, UCLA, Los Angeles, CA, 1999.

- [6] F. Yang and Y. Rahmat-Samii, "Mutual coupling reduction of microstrip antennas using electromagnetic band-gap Structure," *IEEE Antennas and Propagation Society Intl. Symp.*, vol. 2, pp. 478-481, July 2001.
- [7] W.E. III. McKinzie III, R.B. Hurtado, B.K. Klimczak and J.D. Dutton, "Mitigation of multipath through the use of artificial magnetic conductor for precision GPS surveying antenna," *IEEE AP-S Intl. Symp.*, vol. 4, pp. 640-643, June 2002.
- [8] K.M.K.H. Leong, A.C. Guyette, B. Elamaram, W.A. Shiroma and T. Itoch, "Coupling suppression in microstrip lines using a bi-periodically perforated ground plane", *IEEE Microwave and Wireless Components Lett.*, vol. 12, no. 5, pp. 169-171, May 2002.
- [9] R.F. Jimenez Broas, D.F. Sievenpiper and E. Yabolonovitch, "A high-impedance ground plane applied to a cellphone handset geometry," *IEEE Trans. Microwave Theory and Tech.*, vol. 49, no. 7, pp. 1262-1265, Jul. 2001.
- [10] S. Rogers, W. McKinzie and G. Mendolia, Artificial Magnetic Conductor (AMC) technology enables the coexistence of 802.11b and Bluetooth™, Technical literature Etenna Corporation.
- [11] T. Kamgaing, High-impedance electromagnetic surfaces for mitigation of simultaneous switching noise in high-speed circuits, Ph.D. Thesis, Department of Electrical Engineering, UMD, College Park, MD, 2003.
- [12] T. Kamgaing and O.M. Ramahi, "A novel power plane with integrated simultaneous switching noise mitigation capability using high-impedance

- surfaces,” *IEEE Microwave and Wireless Components Lett.*, vol. 13, no. 1, pp. 21-23, Jan. 2003.
- [13] S. Shahparnia and O.M. Ramahi, “Electromagnetic interference (EMI) reduction from printed circuit boards (PCB) using electromagnetic bandgap structures,” accepted for publication in *IEEE Transactions on Electromagnetic Compatibility*.
- [14] T. Kamgaing and O.M. Ramahi, “Inductance-enhanced high-impedance surfaces for broadband simultaneous switching noise mitigation in power planes,” *IEEE MTT-S International, Microwave Symposium Digest*, vol. 3, pp. 2165-2168, June 2003.
- [15] R. Abhari and G.V. Eleftheriades, “Metallo-dielectric electromagnetic bandgap structures for suppression and isolation of the parallel-plate noise in high-speed circuits,” *IEEE Trans. on Microwave Theory and Techniques*, vol. 51, no. 6, pp. 1629-1639, June 2003.
- [16] Y.J. Wang, W.J. Koh, C.K. Lee and K.Y. See, “Electromagnetic coupling analysis of transient signal through slots or apertures perforated in a shielding metallic enclosure using FDTD methodology,” *Progress In Electromagnetic Research*, PIER 36, pp. 247-264, 2002.
- [17] I. Belokour, J. LoVetri and S. Kashyap, “Shielding effectiveness estimation of enclosure with aperture,” *IEEE Electromagn. Compatibility Intl Symp.*, vol. 2, pp. 855-860, Aug. 2000.
- [18] F. Olyslager, E. Laermans, D. De Zutter, S. Criel, R. De Smedt, N. Lietaert and A. De Clercq, “Numerical and experimental study of the shielding effectiveness

- of a metallic enclosure,” *IEEE Trans. Electromagn. Compatibility*, vol. 41, no. 3, pp. 202-213, Aug. 1999.
- [19] J. J. Burke and R. W. Jackson, “Reduction of parasitic coupling in packaged MMICs”, *IEEE MTT-S Digest*, vol. 1, pp. 255-258, May 1990.
- [20] Lin Li and O.M. Ramahi, “Analysis and reduction of electromagnetic field leakage through loaded apertures,” *IEEE International Symposium on Antennas and Propagation Society International Symposium*, vol. 3, pp. 102-105, June 2002.
- [21] A. Aminian, F. Yang and Y. Rahmat-Samii, “In-phase reflection and EM wave suppression characteristics of electromagnetic band gap ground planes,” *IEEE Proc. Antennas and Propagation Society International Symposium*, vol. 4, pp. 430-433, June 2003.
- [22] R. Coccioli, Fei-Ran Yang, Kuang-Ping Ma and T. Itoh, “Aperture-coupled patch antenna on UC-PBG substrate,” *IEEE Trans. Microwave Theory and Tech.*, vol. 47, no. 11, pp. 2123-2130, Nov. 1999.
- [23] S. Shahparnia and O.M. Ramahi, “Simultaneous switching noise mitigation in PCB using cascaded high-impedance surfaces,” *IEEE Electronics Letters*, vol. 40, no. 2, pp. 98-100, Jan. 2004.
- [24] M. Omiya, T. Hikage, N. Ohno, K. Horiguchi, and K. Itoh, “Design of cavity-backed slot antennas using the finite-difference time-domain technique,” *IEEE Trans. Antennas Propagat.*, vol. 46, pp. 1853-1858, Dec. 1998.



- [25] C.J. Reddy, M.D. Deshpande and D.T. Fralick, Analysis of elliptically polarized cavity backed antenna using a combined FEM/MOM/GTD technique, NASA Contractor Report 198197, Aug. 1995.
- [26] C.J. Reddy, M.D. Deshpande, C.R. Cockrell and F.B. Beck, "Radiation characteristics of cavity backed aperture antenna in finite ground plane using the hybrid FEM/MOM technique and geometrical theory of diffraction," *IEEE Trans. Antennas Propagat.*, vol. 44, no. 10, pp. 1327-1333, Oct. 1996.
- [27] D. Sievenpiper, L. Zhang, R.F.J. Broas, N.G. Alexopolous and E. Yablonovitch, "High impedance electromagnetic surfaces with a forbidden frequency band," *IEEE Transactions on Microwave Theory and Techniques*, vol. 47, no. 11, pp. 2059-2074, Nov. 1999.
- [28] D. Sievenpiper and E. Yablonovitch, "Eliminating surface currents with metallodielectric photonic crystals," *IEEE Proc. MTT-S International Microwave Symposium*, vol. 2, pp. 663-666, June 1998.
- [29] L. Brillouin, Wave propagation in periodic structures, Electric Filters and Crystal Lattices, McGraw-Hill, 1946.
- [30] D.M. Pozar, "Input impedance and mutual coupling of rectangular microstrip antennas," *IEEE Trans. Antennas Propagat.*, vol. 30, pp. 1191-1196, Nov. 1982.